CtIP-mediated alternative mRNA splicing fine-tunes the DNA damage response

ROSARIO PRADOS-CARVAJAL,[1,2,3] GUILLERMO RODRÍGUEZ-REAL,[1,2] GABRIEL GUTIERREZ-POZO,[1] and PABLO HUERTAS[1,2]

[1]Departamento de Genética, Universidad de Sevilla, Sevilla, 41080, Spain

[2]Centro Andaluz de Biología Molecular y Medicina Regenerativa-CABIMER, Universidad de Sevilla-CSIC-Universidad Pablo de Olavide, Sevilla, 41092, Spain

ABSTRACT

In order to survive to the exposure of DNA damaging agents, cells activate a complex response that coordinates the cellular metabolism, cell cycle progression, and DNA repair. Among many other events, recent evidence has described global changes in mRNA splicing in cells treated with genotoxic agents. Here, we explore further this DNA damage-dependent alternative splicing. Indeed, we show that both the splicing factor SF3B2 and the repair protein CtIP contribute to the global pattern of splicing both in cells treated or not to DNA damaging agents. Additionally, we focus on a specific DNA damage- and CtIP-dependent alternative splicing event of the helicase PIF1 and explore its relevance for the survival of cells upon exposure to ionizing radiation. Indeed, we describe how the nuclear, active form of PIF1 is substituted by a splicing variant, named vPIF1, in a fashion that requires both the presence of DNA damage and CtIP. Interestingly, timely expression of vPIF1 is required for optimal survival to exposure to DNA damaging agents, but early expression of this isoform delays early events of the DNA damage response. On the contrary, expression of the full length PIF1 facilitates those early events but increases the sensitivity to DNA damaging agents if the expression is maintained long-term.

Keywords: CtIP; SF3B complex; PIF1; DNA damage response; mRNA splicing

INTRODUCTION

DNA is constantly threatened by endogenous and external sources that compromise its integrity. Thus, during evolution eukaryotes have developed a complex signaling network that fine-tunes the response to those threats. Generally referred to as the DNA Damage Response (DDR), such a network affects virtually every aspect of the cell metabolism (Jackson and Bartek 2009; Ciccia and Elledge 2010). In addition to those changes, the DDR activates the actual repair of damaged DNA. There are many different DNA lesions, thus several specific repair pathways coexist. DNA double strand breaks (DSBs) are the most cytotoxic form of DNA damage. Indeed, repair of DSBs can be achieved by different mechanisms, generally grouped in two categories, regarding the use or not of a template for repair. Whereas nonhomologous end-joining (NHEJ) uses no homology with seal DSBs, homologous recombination will copy the information from a homologous sequence (Lieber 2010; Jasin and Rothstein 2013). The decision between those pathways is controlled by the DDR and relies on the activation or not of the processing of the DNA ends, the so-called DNA end resection (Symington et al. 2014). This regulation is mostly achieved by controlling a single protein, CtIP, which integrates multiple signals in order to activate or not end processing (Symington et al. 2014; Makharashvili and Paull 2015). Thus, in order to modulate resection and, as a consequence, homologous recombination, CtIP works together with several other proteins that affect the processivity of the end resection, mainly the tumor suppressor gene BRCA1 (Cruz-García et al. 2014).

Recently, a crosstalk between the DDR and the RNA metabolism at different levels has been discovered. Indeed, the number of factors that participate in the DNA damage response and/or are regulated by it has expanded considerably in recent years to include many RNA-related proteins, notably splicing and alternative splicing factors (Jimeno et al. 2019; Nimeth et al. 2020). So, post-

[3]**Present address:** DDR Biology, Bioscience; Oncology R&D, AstraZeneca, Cambridge, United Kingdom

Corresponding author: pablo.huertas@cabimer.es

Article is online at http://www.rnajournal.org/cgi/doi/10.1261/rna.078519.120.

translational changes of splicing factors following DNA damage such as phosphorylation, ubiquitination, sumoylation, neddylation, PARylation, acetylation, and methylation of splicing factors, have been documented. On the other hand, bona fide DDR factors also directly control splicing. For example, BRCA1 regulates alternative splicing in response to DSB formation through its DNA damage-dependent interaction with several splicing factors such as SF3B1, one of the subunits of the Splicing Factor 3B (SF3B) complex (Savage et al. 2014). SF3B is a multiprotein complex essential for the accurate excision of introns from premessenger RNA (Golas et al. 2003). This complex consists of seven subunits: SF3B1 (also known as SF3b155), SF3B2 (SF3b145), SF3B3 (SF3b130), SF3B4 (SF3b49), SF3B5 (SF3b10), SF3B6 (SF314a), and SF3B7 (PHF5a) (Spadaccini et al. 2006). SF3B plays an indispensable role during the assembly of the prespliceosome recognizing the intron's branch point (Teng et al. 2017). Interestingly, several subunits of this complex have been found in genome-wide screens for factors involved in DNA repair, affecting homologous recombination (Adamson et al. 2012), controlling genome stability (Paulsen et al. 2009), or as substrates of the checkpoint kinases (Matsuoka et al. 2007). Moreover, we recently reported that the SF3B complex directly interacts with CtIP and regulates its activity in DNA end resection (Prados-Carvajal et al. 2018).

Interestingly, in addition to its well-defined role in DSB repair by regulating DNA end resection, CtIP seems to perform many additional tasks in the cell, affecting DNA repair, cell cycle progression, checkpoint activation, replication, and transcription (Liu and Lee 2006; Wu and Lee 2006; Duquette et al. 2012; Moiola et al. 2012; Makharashvili and Paull 2015). CtIP promotes the expression of several genes, such as Cyclin D1, and also activates its own promoter (Liu and Lee 2006). The role of CtIP in regulating gene expression is confirmed by its interaction with other transcriptional factors like IIKZF1, TRIB3, and LMO4 (Koipally and Georgopoulos 2002; Sum et al. 2002; Xu et al. 2007). Also, CtIP contributes to DNA damage-dependent cell cycle arrest in S and G2 phases promoting p21 transcription (Li et al. 1999; Liu et al. 2014) and up-regulating the expression of GADD45A (Liao et al. 2010). Additionally, CtIP has been reported to regulate R-loop biology. CtIP deficiency has been shown to promote the accumulation of stalled RNA polymerase and DNA:RNA hybrids at sites of highly expressed genes (Makharashvili et al. 2018). On the contrary, CtIP depletion reduces DNA:RNA hybrid accumulation dependent on de novo transcription of dilncRNA (damage-induced long noncoding RNAs) starting at DSBs (D'Alessandro et al. 2018). Hence, CtIP loss seems to increase R-loops that are produced as a consequence of previous transcription and appears to decrease de novo production of diRNAs (DSB-induced small RNA), thus reducing the DNA:RNA hybrids formed after DNA damage.

Hence, CtIP has a central role in the DDR and DNA repair but plays additional roles in RNA biology. As mentioned before, it physically interacts with the SF3B splicing complex (Prados-Carvajal et al. 2018). Thus, we wondered whether the CtIP–SF3B functional relationship might extend to controlling mRNA splicing and, more specifically, DNA damage-induced alternative splicing. Here we show that both SF3B and CtIP, albeit in a more modest manner, influence expression and splicing of hundreds of genes. This effect is visible in unchallenged cells, but more evident when cells have been exposed to a DNA damaging agent. Then, we analyzed in detail the effect of a DNA damage- and CtIP-dependent alternative splicing event of the helicase PIF1. Although PIF1 and CtIP also interact directly and are involved in DNA end resection (Jimeno et al. 2018a), we observed that such alternative splicing of PIF1 is not involved in DNA end processing, but it affects the cell survival upon exposure to DNA damaging agents. Interestingly, this alternative PIF1 form, when expressed constitutively, hampers the recruitment of DSB repair proteins at early time points but makes cells hyper-resistant to treatments with camptothecin.

RESULTS

SF3B controls DNA damage-induced alternative splicing

As mentioned in the introduction, SF3B controls HR and DNA end resection (Prados-Carvajal et al. 2018). Whereas the resection phenotype was completely dependent on regulation of CtIP, our data suggested other, CtIP-independent, roles of SF3B in DNA repair (Prados-Carvajal et al. 2018). Due to the well stablished role of SF3B in splicing (Sun 2020) and, particularly its implication in DNA damage-dependent alternative splicing (Savage et al. 2014), we decided to analyze this role in more detail. Thus, we carried out a splicing microarray Transcriptome Arrays HTA & MTA using both damaged (6 h after 10 Gy of irradiation) or untreated cells that were depleted or not for SF3B2 using shRNA (Fig. 1A; see Materials and Methods for details). As previously published, SF3B2 depletion affects CtIP protein levels slightly (Prados-Carvajal et al. 2018). Such an array allows the genome-wide study of RNA expression and RNA splicing simultaneously. As SF3B2 controls the levels of CtIP and BRCA1 mRNA (Prados-Carvajal et al. 2018), we first focused on total RNA levels genome-wide. Changes were considered significant when the fold change (FC) was two or more and the *P*-value less than 0.05. Indeed, SF3B2 depletion using shRNA leads to the specific up-regulation of 52 genes solely in undamaged conditions when compared with control cells (Fig. 1B). Moreover, 26 genes were exclusively overexpressed in SF3B2 down-regulated cells upon exposure to DNA damage (Fig. 1B). Additionally, mRNAs abundance from 27 genes was increased in cells

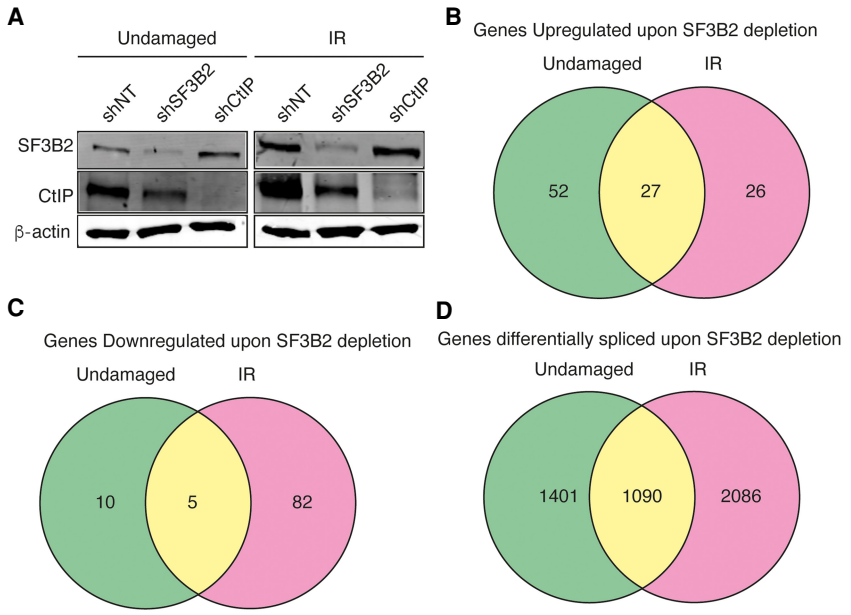

FIGURE 1. SF3B2 depletion affects gene expression and splicing of many genes. (*A*) Representative western blot showing the expression levels of SF3B2 and CtIP upon depletion with the indicated shRNAs in cells exposed or not to 10 Gy of ionizing radiation. α-tubulin blot was used as loading control. (*B*) Distribution of the genes up-regulated upon SF3B2 depletion regarding the exposure or not to DNA damage. Fold change (FC) > 2, *P*-value < 0.05. Gene expression was measured using the GeneChip HTA Array as described in the Materials and Methods section. The number of up-regulated genes in undamaged cells (green), 6 h after exposure to irradiation (10 Gy; pink) or both (yellow) is shown in a Venn diagram. The actual list of genes can be found in Table 1. (*C*) Same as *A* but for down-regulated genes. The actual list of genes can be found in Table 2. (*D*) The GeneChip HTA Array was used to look for genes that changed their splicing upon SF3B2 depletion, as mentioned in the Materials and Methods section. Other details as in *A*. The actual list of genes can be found in Supplemental Table 1.

with reduced SF3B2 levels in both damaged and undamaged cells (Fig. 1B). A list of those genes could be found in Table 1. On the other hand, SF3B2 depletion also reduced expression of 97 genes (Table 2; Fig. 1C). Only 10 of those genes were down-regulated specifically in unperturbed conditions, 82 in cells that were exposed to ionizing radiation and five in both conditions, including SF3B2 itself as expected due to the shRNA-induced down-regulation (Table 2; Fig. 1C).

In terms of mRNA splicing, we confirmed that both depletion of SF3B2 with shRNA and DNA damage induction affect such RNA processing globally. We first calculated the splicing index of exons on all four conditions and compared them in silico (FC > 2, *P*-value < 0.05; see Materials and Methods for additional details). The results are summarized in Figure 1C and a list of genes can be found in Supplemental Table S1. More than 4500 genes were differentially spliced when SF3B2 was absent, compared with a nontargeted shRNA (Fig. 1D). Almost 25% did so regardless of the presence or absence of an exogenous source of DNA damage (yellow), but almost 45% showed splicing events that were both DNA damage- and SF3B-dependent (red) and only 30% of the genes were spliced by SF3B in undamaged conditions (green). Thus, most of the splicing events that require SF3B2 happens in damaged samples, indicating that this factor is especially relevant in stress conditions.

Indeed, a different analysis considering all genes that show an alternative splicing upon irradiation (IR) indicates that only 14% did so both in control and in SF3B2 depleted cells, whereas 46% of the genes suffer DNA damage-induced alternative splicing only when SF3B2 was present, suggesting they require this factor for such an event. Strikingly, an additional 40% of the genes suffer damage induced alternative splicing specifically in SF3B2 depleted cells, indicating that when the SF3B complex was absent the splicing landscape is severely affected, and new events appear.

Interestingly, the pattern of gain (+) or loss (−) of specific events of alternative splicing was similar in all situations (Table 3) with the exception of SF3B2-depleted cells upon irradiation, that was more pronounced in agreement with a strong role of the SF3B complex in DNA damage-induced alternative splicing (Savage et al. 2014). Despite the strong quantitative difference in splicing, qualitatively the types of events were similarly distributed in all cases (Table 3).

In order to validate the array, we studied the mRNA level of several splicing variants of genes that were identified as positives in the analysis. Due to our interest, we focused mainly on those that are related to DNA resection, recombination, or the DNA damage response. To do so, we depleted SF3B2 using siRNA and induced or not DNA damage (10 Gy irradiation; Fig. 2A). Cells were incubated for 6 h to allow accumulation of DNA damage-dependent isoforms. We used qPCR and sets of isoform-specific primers (Table 4) to study the level of different variants. In all cases, we included an analysis of a "common isoform" that is present ubiquitously in all conditions. The ratio between the alternative variant and the "common isoform" was normalized to control cells, that is, nonirradiated cells transfected with nontargeted siRNA. As shown in Figure 2B, the levels of a specific *BRCA1* isoform increased upon DNA damage, but SF3B2 depletion blocks the accumulation of such *BRCA1* mRNA specie even in untreated cells. Thus, we described a SF3B2- and DNA-damage induced splicing variant of this

TABLE 1. Genes up-regulated upon SF3B2 depletion

Genes up-regulated in undamaged cells	Genes up-regulated in damaged cells	Genes up-regulated in undamaged and damaged cells
ABCA5	ANKRD18DP	BET1
AC087073.1	ANKRD45	C12orf39
ANTXR2	CCDC30	CBWD1
ATG12	CHKA	CBWD2
C14orf37	CTD-2651B20.3	CBWD3
C1orf168	EIF5	CBWD6
C1orf63	GABRR3	CBWD7
C21orf91	HAVCR2	CDO1
C9orf156	JAKMIP1	CGRRF1
CCDC66	KLHL41	CTD-2023N9.3
CD274	NME8	FAM133B
CDKN1B	PDE4D	FLVCR1
CREBRF	RP11-386I8.6	GMFB
DNAJC27	RP11-473L15.3	KDM3A
DTD2	RP11-545I10.2	MITD1
ENOX1	RP4-553F4.6	MMP13
FBXW7	RRH	MTHFD2L
GBP1	SLFN12	NPM3
GDAP1	SPATA9	NQO1
GTF2E2	SYNE1	RP11-111F5.3
HEBP1	THEMIS	RSAD2
HSD17B13	TRAM1	SPHAR
IKZF3	TSPY5P	SRD5A3-AS1
IL18R1	WDR87	STARD4
IL5	ZNF442	TULP3
ITPR2	ZNF571	TXNDC2
KANSL2		ZNF844
KIAA1467		
MAGOH		
METTL13		
NCAPG2		
PARP16		
PCNXL2		
PDIK1L		
PPARGC1A		
RP11-159G9.5		
RP11-213G2.2		
RP11-261C10.3		
RP11-46C20.1		
RP13-996F3.4		
S100A8		
SCO1		
SESN1		
SLC25A27		
SRPRB		
SUN3		
THOC7		
TP53INP1		
TRPM7		
USP54		
ZMAT3		
ZNF669		

TABLE 2. Genes down-regulated upon SF3B2 depletion

Genes down-regulated in undamaged cells	Genes down-regulated in damaged cells	Genes down-regulated in undamaged and damaged cells
AHCYL1	GRAP	CAV1
AL603965.1	KRT27	EXOSC3
ALDH1L1	LINC00482	KDELC2
ALPL	OR6T1	NID1
ANO1	PRSS22	ST3GAL5
ANXA8	RP1-300G12.2	
ANXA8L1	RP11-429E11.2	
ARHGAP31	SNCAIP	
ATG5	SPINK14	
BCL2A1	VPS37C	
BECN1		
C12orf50		
C14orf182		
CCL2		
CCL7		
CCNDBP1		
CDC45		
CHORDC1		
CLMP		
CSF2		
CTC-436P18.3		
CYB5R2		
E2F1		
FAM49A		
FANCD2		
GALNT1		
GINS1		
HSPB11		
IARS		
ICAM1		
INPP5B		
ITGB3		
KCNH7		
KCNMA1		
KIAA1279		
KLHDC3		
KRT20		
KRT6A		
KRT6C		
KRT75		
LGI2		
LRFN5		
LRRC15		
MBNL2		
MMP9		
MOCOS		
MYH16		
NCEH1		

Continued

TABLE 2. *Continued*

Genes down-regulated in undamaged cells	Genes down-regulated in damaged cells	Genes down-regulated in undamaged and damaged cells
NDUFS3		
NEK7		
NMD3		
PALM3		
PAPOLA		
PDE9A		
PEPD		
PIEZO2		
PIR		
PLA2G7		
PLOD2		
PPP4R4		
PRLR		
QRFPR		
RCAN2		
RP11-1152H15.1		
RP11-18H21.1		
RP11-283G6.5		
RP11-295K2.3		
RP11-47I22.3		
RP3-522D1.1		
RP5-968D22.1		
SF3B2		
SGK196		
SLC22A4		
SLCO2A1		
SSTR2		
ST6GALNAC3		
THBS1		
TNFRSF9		
TOMM34		
TPK1		
TPPP3		
WAC-AS1		

mRNA. Differently, we confirmed that *RAD51* and *EXO1* have a damaged-dependent isoform that is independent of SF3B2 (Fig. 2C,D). Also, in agreement with the array data, the levels of a *DNA2* mRNA variant increased specifically with DNA damage in the absence of SF3B2 (Fig. 2E). *PIF1* mRNA alternative isoform expression increased both upon irradiation and upon SF3B2 depletion in an epistatic manner (Fig. 2F). Finally, we studied *ATR*, whose alternative splicing is dependent on SF3B2 regardless the presence or absence of DNA damage (Fig. 2G). In summary, in agreement with the array, SF3B complex and/or DNA damage presence controls the alternative splicing of DNA repair factors.

CtIP controls mRNA expression and splicing of several genes

As mentioned previously, SF3B directly interacts and regulates the resection factor CtIP. Interestingly, CtIP is a multifunctional protein that works in DNA repair, but also in other processes, including transcription (Wu and Lee 2006). Moreover, other proteins related to DNA end resection, such as BRCA1, also have a role in RNA metabolism (Kleiman et al. 2005; Veras et al. 2009). Thus, we wondered whether CtIP could also play a role in RNA splicing due to its connection with SF3B. To test this idea, and as for SF3B2, we used the splicing microarray to analyze RNA

TABLE 3. Specific splicing changes in response to IR and SF3B2 depletion

Comparison	Irradiated versus nonirradiated samples in control cells	Irradiated versus nonirradiated samples in SF3B2 depleted cells	SF3B2 depleted versus control cells in untreated conditions	SF3B2 depleted versus control cells in irradiated conditions
(+) Alt-carboxyl terminus	274	220	201	375
(+) Alt-amino terminus	265	215	185	335
(+) Alt-coding	39	44	35	53
(+) Nonsense mediated decay	72	53	59	117
(+) Retained intron	75	67	62	122
(+) Truncated	43	52	54	115
(–) Alt-carboxyl terminus	228	234	231	503
(–) Alt-amino terminus	245	249	222	479
(–) Alt-coding	42	53	93	164
(–) Nonsense mediated decay	44	44	77	152
(–) Retained intron	61	68	76	175
(–) Truncated	63	56	28	66

(+) represents gain and (–) loss of each specific event.

abundance and splicing genome-wide in cells depleted or not for CtIP using an shRNA, both in damaged and untreated conditions (Fig. 1A for depletion of CtIP). When studying genome-wide expression levels of human genes, we observed that upon depletion of CtIP, and despite the assigned function in transcription, only 74 mRNAs showed altered abundance: 36 were up-regulated and 38 down-regulated (Tables 5, 6; Fig. 3A,B; Note that CtIP itself is among the down-regulated ones, as expected due to the effect of the shRNA). Only 12 genes were exclusively up-regulated in cells exposed to IR in cells depleted for CtIP compared with control cells (Table 5; Fig. 3A). However, in undamaged conditions solely 22 genes were up-regulated and the levels of only two genes increased in both conditions, with and without damage, in cells down-regulated for CtIP (Table 5; Fig. 3A). On the other hand, CtIP knockdown reduced the expression of 16 genes exclusively in unperturbed cells whereas the expression of 18 genes were decreased in irradiated cells (Table 6; Fig. 3B). The expression of only four genes was down-regulated upon CtIP depletion in both damaged and undamaged cells (Table 6; Fig. 3B).

Additionally, we studied mRNA splicing in the same conditions mentioned above and, interestingly, we realized that the down-regulation of CtIP rendered a strong effect on RNA processing of hundreds of genes. As shown in Table 7, columns 4 and 5, CtIP down-regulation on its own changed the pattern of mRNA splicing compared to control conditions, even though this phenotype was more pronounced in unperturbed cells.

As CtIP and SF3B2 physically interact, we wondered how many of the events that show a CtIP-dependent splicing did also rely on SF3B2 for that process, regardless of the exposure or not to DNA damage (Fig. 3C). As expected, the number of splicing events that were dependent on SF3B2, a bona fide splicing factor, was higher than those that require CtIP. Indeed, only <30% of those SF3B2-dependent events were diminished upon CtIP depletion. But interestingly, around 70% of the CtIP-dependent splicing events were also affected by SF3B2. Thus, our results suggest that CtIP has a role in splicing, although less prominent than SF3B2. Moreover, most CtIP-dependent splicing events require also the SF3B complex, reinforcing the idea that CtIP might usually act with SF3B during splicing regulation, regardless of the fact that there are also a minority of CtIP-dependent but SF3B2-independent specific splicing events. On the contrary, SF3B can readily act on the splicing of most genes independently of CtIP.

Considering the role of CtIP in the response to DNA damage, we decided to simultaneously analyze the effect of CtIP depletion and irradiation on genome-wide alternative splicing. Thus, we carried out another analysis in which

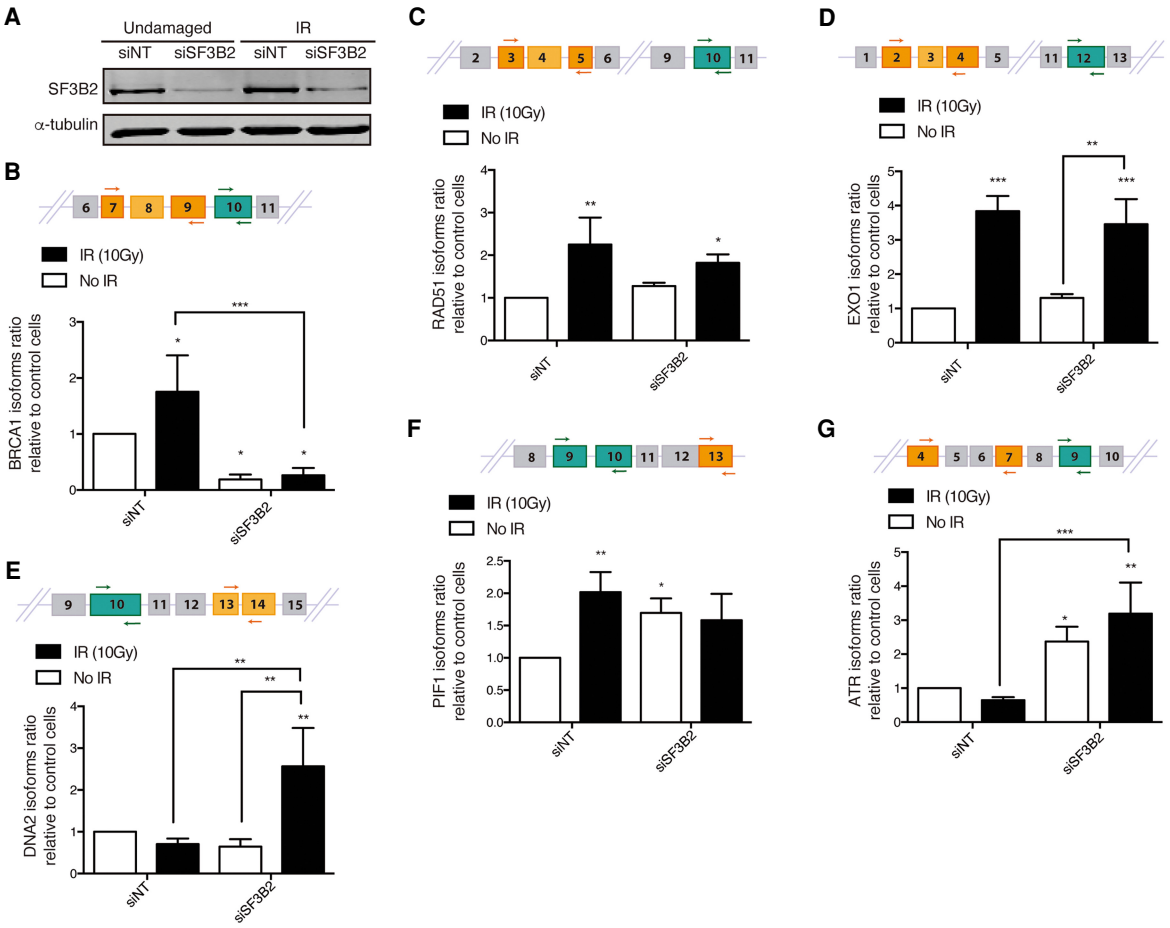

FIGURE 2. Splicing changes in DDR factors in cells depleted for SF3B2. (*A*) Representative western blot showing the expression levels of SF3B2 upon depletion with a siRNA against SF3B2 or a control sequence (siNT) in cells exposed or not to 10 Gy of ionizing radiation. α-tubulin blot was used as loading control. (*B–G*) Specific RNA isoforms levels of the indicated genes were calculated as the ratio between the abundance of the specific splicing form normalized with the total amount of each gene RNA by quantitative RT-PCR using specific primers in cells transfected with the indicated siRNAs and 6 h after irradiation or mock treatment. See Materials and Methods for details. A schematic representation of the splicing events measured is shown in each case on the *top*. The common splicing event analyzed is shown in green, oligos are represented as arrows. The specific splicing that changes upon SF3B2 depletion is shown in orange. The graphs represent the average and standard deviation of three independent experiments. Statistical significance was calculated using an ANOVA test. (*) $P < 0.05$, (**) $P < 0.01$, and (***) $P < 0.005$.

we compared all conditions in pairs: control cells without DNA damage (shNT) or exposed to IR (shNT6h) or depleted for CtIP in unperturbed (shCtIP) or damaged cells (shCtIP6h) (Fig. 3D). Only 107 genes were altered due to CtIP absence in irradiated cells, whereas 205 did so in undamaged cells (Fig. 3D; in green and blue, respectively). The splicing of 494 genes was changed specifically in response to DNA damage exclusively in CtIP depleted cells (Fig. 3D, in red). In a similar number of genes (423 genes; Fig. 3D, yellow), mRNA splicing was modified in response to DNA damage only in cells that retained CtIP. We were particularly interested in those latter mRNA, as they represented DNA damage-dependent mRNA variants that are CtIP dependent. Hence, we reasoned that CtIP might mediate, directly or indirectly, such DNA damage-dependent alternative mRNA processing. Among them, we found that CtIP controls the DNA damage-dependent splicing of the helicase PIF1. Interestingly, SF3B2 also affects PIF1 splicing (Fig. 2F). Strikingly, PIF1 and CtIP physically interact and together contribute to DNA end resection over specific DNA structures such as G-quadruplexes (Jimeno et al. 2018b). Thus, in order to study deeply the crosstalk between CtIP, DNA end resection, and RNA splicing, we decided to focus on the altered splicing of PIF1.

CtIP controls mRNA splicing of *PIF1*

PIF1 is a helicase with a 5′–3′ polarity. In humans there is only one PIF1 gene, but it was known to produce two well-studied different transcripts (Supplemental Fig. 1A). A short transcript (2295 nt) produces the longer protein isoform (707 aa) called PIF1ß, which is located in the mitochondria. On the other hand, the longer transcript (2688 nt) is translated into a smaller protein variant named

TABLE 4. DNA primers

Primer name	Sequence (5′–3′)	Use
ACTB qPCR Fwd	ACGAGGCCCAGAGCAAGA	RT-qPCR of Actin
ACTB qPCR Rvs	GACGATGCCGTGCTCGAT	RT-qPCR of Actin
BRCA1 common isoform Fwd	CCCTTTCACCCATACAC	To validate the microarray of SF3B2 splicing isoforms
BRCA1 common isoform Rvs	AAGTGTTGGAAGCAGG	To validate the microarray of SF3B2 splicing isoforms
RAD51 isoform Fwd	TCCAGAACAGCACCAAAG	To validate the microarray of SF3B2 splicing isoforms
RAD51 isoform Rvs	GTGGTGACTGTTGGAAG	To validate the microarray of SF3B2 splicing isoforms
RAD51 common isoform Fwd	CATVTGGAGGTAGCAGAAG	To validate the microarray of SF3B2 splicing isoforms
RAD51 common isoform Rvs	CTCGTGCTAATCTGGAC	To validate the microarray of SF3B2 splicing isoforms
EXO1 isoform Fwd	CCTCGGAGTGAGAGAAA	To validate the microarray of SF3B2 splicing isoforms
EXO1 isoform Rvs	TGTAGCAATCCCTGTATCCC	To validate the microarray of SF3B2 splicing isoforms
EXO1 common isoform Fwd	CTGAAGTGTTTGTGCCTGAC	To validate the microarray of SF3B2 splicing isoforms
EXO1 common isoform Rvs	CCACAACTGCACCAC	To validate the microarray of SF3B2 splicing isoforms
DNA2 isoform Fwd	CAGAGGCAAGCGATGA	To validate the microarray of SF3B2 splicing isoforms
DNA2 isoform Rvs	AACCACAGGCGGTAGAGA	To validate the microarray of SF3B2 splicing isoforms
DNA2 common isoform Fwd	GGAGAAGAGTGGCAGTT	To validate the microarray of SF3B2 splicing isoforms
DNA2 common isoform Rvs	TCTGTCACCTGCCATTAG	To validate the microarray of SF3B2 splicing isoforms
ATR isoform Fwd	GTCAGGAAGGTCTATGTG	To validate the microarray of SF3B2 splicing isoforms
ATR isoform Rvs	GTCCTTGAAAGTACGG	To validate the microarray of SF3B2 splicing isoforms
ATR common isoform Fwd	CACCACAGGCACAATCA	To validate the microarray of SF3B2 splicing isoforms
ATR common isoform Rvs	TCCACTAACACAACTAGCCC	To validate the microarray of SF3B2 splicing isoforms
2 PIF1 Fwd	TGGTGAAGCGGCCTGTGGA	To validate the microarray of CtIP splicing isoforms
3 PIF1 Rvs	GTGAAGAAGATGCTCTGG	To validate the microarray of CtIP splicing isoforms
4 PIF1 Rvs	AGTGAGCCCAGGATTCGCTT	To validate the microarray of CtIP splicing isoforms
8 PIF1 Fwd	GTGTTCAGATGAGGTGAC	To validate the microarray of CtIP splicing isoforms
9 PIF1 Rvs	TAGTTGAAGGAGCTGG	To validate the microarray of CtIP splicing isoforms
10 PIF1 Rvs	CTGCCTCGAACCCAAC	To validate the microarray of CtIP splicing isoforms

PIF1α (641 aa) that is localized in the nucleus (Futami et al. 2007). The difference between both proteins is the presence of a mitochondrial localization domain in PIF1ß, which also lacks the signal to translocate into the nucleus. Additionally, other alternative spliced forms have been proposed to exist (Supplemental Fig. 1B). Our array will analyze those forms (Supplemental Fig. 1B), but also any additional inclusion/exclusion of exons or introns. Indeed, our data suggested additional splicing changes on the PIF1α backbone that were CtIP- and DNA damage-dependent (Fig. 4A). We studied the inclusion of exon 3 (Fig. 4A [I]), exon 4 (Fig. 4A [II]), exon 9 (Fig. 4A [III]), and exon 10 (Fig. 4A [IV]). All of these optional events are combinatorial and not mutually exclusive, so a mix of all the possible different species of mRNA coexist in all conditions, regardless of CtIP or DNA damage, but the array predicts changes on different conditions. We studied the abundance of the different alternative events by qPCR in cells depleted or not for CtIP with an siRNA and exposed or not to 10 Gy of ionizing radiation (Fig. 4B–G). The presence of an exon 2–3 junction was only slightly increased upon irradiation or CtIP depletion, but the changes were not significant (Fig. 4C). A similar, but in this case significant, change was observed for the exon 4 inclusion event (Fig. 4D). Exon 8–9 junction presence was strongly increased in response to irradiation in control cells, and both its inclusion and DNA damage-accrue was completely dependent on CtIP presence (Fig. 4E). Exon 10 inclusion event in the mRNA analysis rendered no statistically significant changes in any conditions (Fig. 4F). These results suggested that the clearest CtIP-dependent alternative events in response to exogenous damage occur in the exon 4 inclusion and, more specially, in the exon 8–9 junction of the *PIF1* gene. Interestingly, *PIF1* mRNA splicing was also affected upon SF3B2 depletion (Fig. 2F), although in this case we had analyzed the effect on the exon 9–10 junction as it was the prominent change observed in the array. In order to test if the 8–9 junction of PIF1 was also controlled by SF3B2 and if such an effect was similar to CtIP, we repeated the qPCR experiments using the specific pair of oligos. Strikingly, the DNA damage-induced increase in the 8–9 junction of PIF1 was also controlled by SF3B2 (Fig. 4G), but in a fashion that did not resemble the regulation by CtIP (Fig. 4E) but the effect of SF3B2 on PIF1 exon 9–10 junction (Fig. 2F). That is, the depletion of SF3B2, instead of reducing this event like CtIP, generally increased it.

TABLE 5. Genes up-regulated upon CtIP depletion

Genes up-regulated in undamaged cells	Genes up-regulated in damaged cells	Genes up-regulated in undamaged and damaged cells
AC010967.2	AC068535.3	MMP13
AC016582.2	ADAMTS9	TULP3
AC064852.4	CD200R1L	
AC073043.2	DMXL2	
AF064858.7	IL10	
ARL14	IL24	
C9orf153	KLHL6	
C9orf156	MMP3	
CBLN2	RP11-445K13.2	
COL10A1	SPATA9	
EGLN1	SRD5A3-AS1	
IKZF3	WDR87	
KRT13		
NCEH1		
PARP16		
PPP2R1B		
PRSS44		
RP11-285B24.1		
RP11-290K4.1		
RP11-300J18.2		
RP11-9G1.3		
RP4-553F4.6		
RP4-650F12.2		
SGIP1		
U51244.2		

However, both CtIP and SF3B2 knockdown abolished the DNA damage-dependent stimulation. Thus, we conclude that both SF3B2 and CtIP are required for the DNA-damage increase in the use of the exons 8 and 9 junction but have opposite effects in unchallenged conditions. To reinforce this idea, we repeated the analysis of the exon 8–9 junction in cells depleted of either factor upon stimulation of DNA damage with the topoisomerase I inhibitor camptothecin (CPT; Fig. 4H). In agreement with our hypothesis, the results were similar to those obtained upon irradiation (compare Fig. 4H with 4E and 4F).

In order to determine which activity of CtIP is involved in the splicing of *PIF1*, we carried out several qPCR to analyze the presence of the 8–9 junction on *PIF1* mRNA, but in cells bearing different mutated versions of CtIP (Fig. 4I). We used GFP-CtIP as control, the resection defective CtIP-T847A, a CDK phosphorylation mutant (Huertas and Jackson 2009) and CtIP-E894A, a sumoylation mutant (Soria-Bretones et al. 2017). Lastly, and considering that BRCA1 interacts with CtIP (Yu et al. 2006) and has been involved in damage-dependent alternative splicing (Savage et al. 2014), we analyzed the expression of *PIF1* exon 8–9 junction in the CtIP-S327A CDK phosphorylation mutant, that does not interact with BRCA1 but still resects albeit at a slower pace (Cruz-García et al. 2014). The data were normalized to the control GFP-CtIP, set as 1. Strikingly, both CDK defective phosphorylation mutants GFP-CtIP-T847A and GFP-CtIP-S327A caused a consistent increase in this splicing event, albeit only statistically significant in the T847A CtIP version (Fig. 4I). This suggested CDK phosphorylation of CtIP inhibits the splicing of, at least, the *PIF1* exon 8–9 junction. This is likely resection independent, as the E894A mutant, a sumoylation defective CtIP that is equally impaired in resection as the T847A mutant, did not share such a phenotype (Fig. 4G). Thus, specific post-transcriptional modifications seem also required for the CtIP role in splicing. Specifically, CDK phosphorylation of CtIP blocks such a role, suggesting that the splicing activity of CtIP happens mainly in G1.

PIF1 splicing variants modulate DNA repair

Taking together these results, we decided to study the relevance of those CtIP- and DNA damage-dependent *PIF1* mRNA splicing events in DNA repair process in human cells. Hence, we created two different *PIF1* splicing variants cDNA constructs (Supplemental Fig. 1C). First, a

TABLE 6. Genes down-regulated upon CtIP depletion

Genes down-regulated in undamaged cells	Genes down-regulated in damaged cells	Genes down-regulated in undamaged and damaged cells
DACT3	C8orf4	CtIP
DRAP1	CCL7	GALNT7
ELOVL7	CD69	OLR1
FGF9	CTGF	SMYD2
LINC00482	CXCL10	
MYOCD	GOLT1A	
NDP	INPP4B	
OR6T1	KAT2B	
RBMS3-AS1	MKX	
RCN2	NINJ1	
RP11-1069G10.1	NTRK3	
SEMA3D	PDCD4	
SEZ6	RP5-1172A22.1	
SMIM12-AS1	RP5-968D22.1	
SNORA38B	S1PR3	
VAV2	SLC22A16	
ZNF571	SYVN1	
	TMEM116	
	TMPRSS15	
	TPPP3	

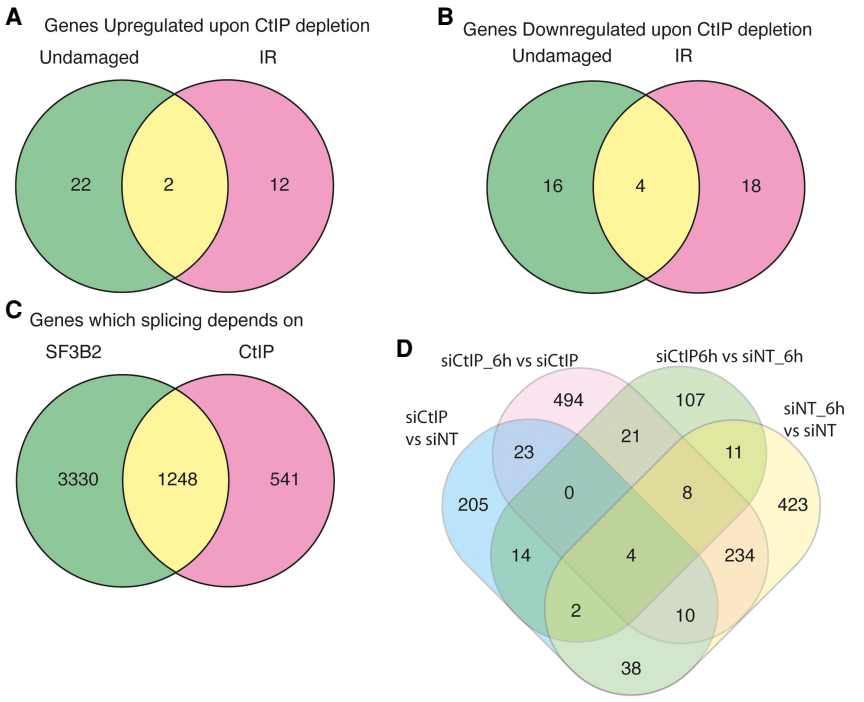

FIGURE 3. CtIP depletion affects gene expression and splicing of many genes. (*A*) Distribution of the genes up-regulated upon CtIP depletion regarding the exposure or not to DNA damage. Fold change (FC) > 2, *P*-value < 0.05. Gene expression was measured using the GeneChip HTA Array as described in the Materials and Methods section. The number of up-regulated genes in undamaged cells (green), 6 h after exposure to irradiation (10 Gy; pink) or both (yellow) is shown in a Venn diagram. The actual list of genes can be found in Table 4. (*B*) Same as *A* but for down-regulated genes. The actual list of genes can be found in Table 5. (*C*) The GeneChip HTA Array was used to look for genes that changed their splicing upon SF3B2 and/or CtIP depletion, as mentioned in the Materials and Methods section. The Venn diagram represents the one that changes when CtIP (pink), SF3B2 (green), or both are down-regulated. Other details as in *A*. (*D*) Differential splicing events bteween different conditions: undamaged cells depleted for CtIP (siCtIP) or transfected with a nontarget siRNA (siNT); or RNA collected 6 h after irradiation in cells depleted for CtIP (siCtIP_6h) or control cells (siNT_6h).

PIF1 containing all exons ("total *PIF1*"; *tPIF1*), which correspond to the canonical PIF1α. In contrast, we also created a *PIF1* variant artificial cDNA that lacks both exon 4 and exon 9, the two exons which inclusion was more dependent on CtIP and DNA damage (Fig. 4C,D). We named it "variant *PIF1*" (*vPIF1*). Importantly, such a construct rendered a PIF1 that lacks part of the helicase domain of the protein. Both genes were expressed from pCDNA. In order to detect the expression of either variant in cells, we tagged both isoforms with GFP. An empty pCDNA plasmid was also used as control in our experiments. We transfected each plasmid (pCDNA, GFP-vPIF1, or GFP-tPIF1) into U2OS in order to study the effect of either isoform in human cells in response to DNA damage. Expression of the proteins coded by those variants is shown in Figure 5A.

Considering that in all the conditions tested for the splicing analysis we could always observe a mixture of different splicing variants, including the canonical PIF1α, we decided to leave the expression of the endogenous *PIF1* gene unperturbed, and combine it with the expression of the different PIF1 variants. First, we analyzed the ability of cells to survive to the DNA damaging agent camptothecin (CPT) when expressing the already spliced vPIF1 and tPIF1 constitutively. Strikingly, constant expression of the tPIF1 rendered cells sensitive to DNA damage when compared with cells expressing the empty plasmid (Fig. 5B). This was not observed when the CtIP- and DNA damage-dependent spliced form vPIF1 was constitutively expressed (Fig. 5B), suggesting that continuous expression of tPIF1 hampers DNA repair and, therefore, agreeing with the idea that a switch from tPIF1 to vPIF1 by DNA damage- and CtIP-induced alternative splicing ensures an adequate response.

Considering the fact that PIF1 and CtIP physically interact and cooperate in DNA end processing (Jimeno et al. 2018b), we decided to study DNA end resection in response to irradiation (10 Gy) in cells expressing either PIF1 construct. However, the overexpression of either isoform caused no effect in DNA resection or the recruitment of the resection and recombination factor BRCA1 (Fig. 5C,D). As a control, we also analyzed the cell cycle in those cells to test whether such overexpression caused any change in the progress of cell cycle (Fig. 5E). The lack of effect on RPA foci formation, an early event, and the timing of the observed splicing changes (6 h after irradiation) suggested that the transition from tPIF1 to vPIF expression might be more relevant for cell survival at later events of the DNA damage response and, therefore, it is separated from the resection role of PIF1.

Early expression of vPIF1 delays DNA repair

In order to understand why changes in *PIF1* splicing to produce vPIF1 was only induced in response to DNA damage and that isoform was not constitutively expressed, we set to analyze the repair of DSBs at early time points in the presence of PIF1 isoforms. Interestingly, we observed that constitutive expression of vPIF1, albeit enhancing the long-term survival in response to DNA damage (Fig. 5B) hampers or delays the recruitment of both NHEJ and

TABLE 7. Specific splicing changes in response to IR and CtIP depletion

Comparison	Irradiated versus nonirradiated samples in control cells	Irradiated versus nonirradiated samples in CtIP depleted cells	CtIP depleted versus control cells in untreated conditions	CtIP depleted versus control cells in irradiated conditions
(+) Alt-carboxyl terminus	274	303	87	44
(+) Alt-amino terminus	265	327	77	46
(+) Alt-coding	39	43	28	7
(+) Nonsense mediated decay	72	63	20	12
(+) Retained intron	75	96	25	11
(+) Truncated	43	46	26	14
(–) Alt-carboxyl terminus	228	282	142	80
(–) Alt-amino terminus	245	298	129	74
(–) Alt-coding	42	44	29	10
(–) Nonsense mediated decay	44	57	36	19
(–) Retained intron	61	83	36	18
(–) Truncated	63	73	15	6

(+) represents gain and (–) loss of each specific event.

HR proteins. Indeed, early after irradiation, the recruitment of the NHEJ factors 53BP1 and RIF1 was mildly impaired (Fig. 6A,B). More strikingly, the recruitment of the essential HR factor RAD51 was severely impaired by constitutive expression of vPIF1 (Fig. 6C). This was not observed when tPIF1 was overexpressed, confirming that this isoform does not block repair. Thus, our data suggest that a timely expression of different isoforms of PIF1 fine-tunes the response to DNA damage. Indeed, it seems that tPIF1 presence is permissive for early events, such as the recruitment of 53BP1, RIF1, or RAD51, but in the long term is deleterious for cell survival in response to DSBs. vPIF1, on the contrary, increases the resistance to DNA damaging agents, despite the fact that expressed too early slows down DSB repair.

Differential localization of PIF1 variants

As mentioned, there are two well-characterized PIF1 isoforms, the nuclear PIF1α and the mitochondrial PIF1β (Supplemental Fig. 1). Although both our constructs, tPIF1 and vPIF1, are based on the nuclear form, PIF1α, we wondered whether vPIF1, which lacks part of the helicase domain, might show a different localization. To test it, we performed a cell fractionation assay. As shown in Figure 7, the protein produced by the tPIF1 construct was mostly chromatin associated as expected (Fig. 7A; green arrow): around 65% in the chromatin-bound and 35% in the cytoplasm (Fig. 7B). On the contrary, the vPIF1 had the opposite distribution (Fig. 7A; red arrow), with 65% of the protein in the cytoplasm and only 35% located in the chromatin fraction (Fig. 7B). Those localizations did not change if cells were exposed to exogenous DNA damage (data not shown).

DISCUSSION

In this work, we have discovered that not only the splicing complex SF3B but also the DNA repair factor CtIP controls the mRNA splicing of several genes, including proteins involved in DDR. Additionally, we have characterized the relevance of some splicing events on *PIF1* gene dependent on CtIP and DNA damage for the DDR and DNA repair.

Our data suggest that the SF3B complex controls the splicing and abundance of different mRNAs, both under unchallenged conditions and especially as a response to DNA damage, as a large set of genes have a differential splicing in SF3B2 depleted cells compared with control cells specifically upon exposure to ionizing irradiation. Interestingly, many of those genes are related to RNA metabolism and protein modifications, known targets of the DNA damage response (Polo and Jackson 2011). These DNA damage-dependent changes in mRNA metabolism

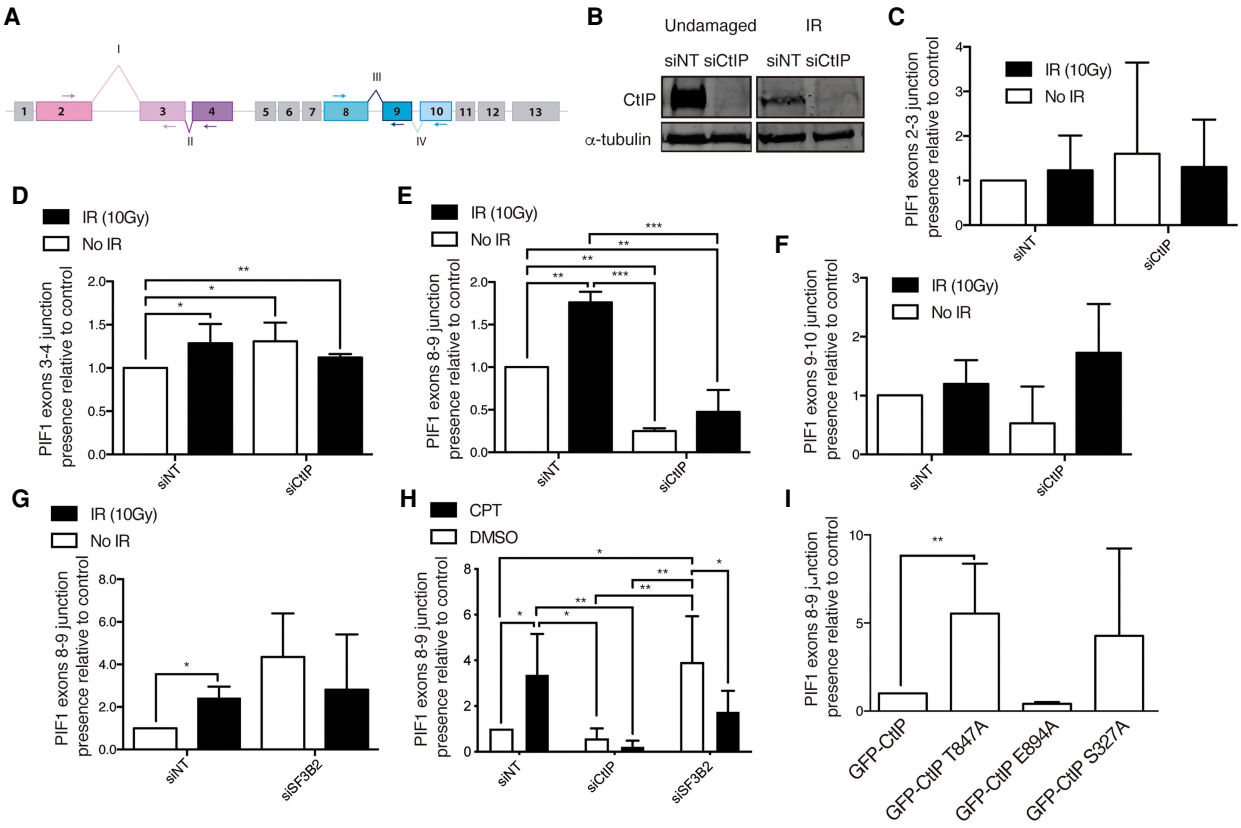

FIGURE 4. PIF1 splicing changes upon CtIP depletion. (*A*) Schematic representation of PIF1 with the exons (boxes) and splicing events analyzed (roman numbers). (*B*) Representative western blots showing the expression levels of CtIP upon depletion with a siRNA against CtIP or a control sequence (siNT) in cells exposed or not to 10 Gy of ionizing radiation. α-tubulin blot was used as loading control. (*C*) Analysis of the exon 2 and exon 3 junctions using quantitative PCR using primers located in exons 2 and 3 (see panel *A*) in cells depleted (siCtIP) or not (siNT) for CtIP, upon exposure to IR (black bars) or in unchallenged conditions (white bars). The data were normalized to the expression of a constitutive exon. The abundance of such events was normalized to the control cells in undamaged conditions. The average and standard deviation of three independent experiments is shown. Statistical significance was calculated using an ANOVA test. (*) $P < 0.05$, (**) $P < 0.01$, and (***) $P < 0.005$. (*D*) Same as *B* but for the inclusion of exon 4. Primers in exons 2 and 4 were used (see panel *A*). Other details as in panel *B*. (*E*) Same as *B* but for the inclusion of exon 9. Primers in exons 8 and 9 were used (see panel *A*). Other details as in panel *B*. (*F*) Same as *B* but for the inclusion of exon 10. Primers in exons 8 and 10 were used (see panel *A*). Other details as in panel *B*. (*G*) Same as *E* but upon depletion of SF3B2 instead of CtIP. (*H*) Same as *E* but upon depletion of either CtIP or SF3B2 as indicated and in cells exposed for 6 h to camptothecin (CPT, black bars) or DMSO (white bars). (*I*) Study of the exon 8–9 junction in cells depleted for endogenous CtIP and expressing the indicated mutants of CtIP. Other details as in panel *B*.

agree with previous studies that reported large changes in mRNA expression (Gasch et al. 2001; Rieger et al. 2004). Additionally, several members of the SF3B complex have been identified by different genome-wide analysis as targets of the DDR (Matsuoka et al. 2007; Bennetzen et al. 2010; Beli et al. 2012; Elia et al. 2015) and DNA damage-dependent splicing events that are specific to certain splicing factors have been previously documented (Shkreta et al. 2016; Cloutier et al. 2018). In the SF3B case, we hypothesize that both aspects, gene expression and splicing changes, are indeed related to the splicing activity of the complex. Although regulation of transcription has been primarily associated for such alterations in gene expression, it has been increasingly clear that post-transcriptional modifications could indeed affect mRNA levels in response to DNA damage. Indeed, up to 50% of the changes on mRNA level in response to genotoxic agents could be attributed to mRNA turnover and not transcription (Fan et al. 2002; Boucas et al. 2012). Alternative splicing is known to affect mRNA stability in response to DNA damage by creating nonproductive transcripts that are subjected to degradation by the nonsense mediated decay pathway (Barbier et al. 2007; Ip et al. 2011). In other cases, direct splicing-dependent gene expression repression or activation in response to DNA damage has been observed (Pleiss et al. 2007; Ip et al. 2011). Along those lines, we propose that alternative splicing controlled by the SF3B complex affects generally expression levels and the accumulation of alternative spliced mRNA in response to DNA damage. This global response will help the cells to fine-tune the response to broken DNA. Additionally, our splicing array data shows that SF3B2 affects also the

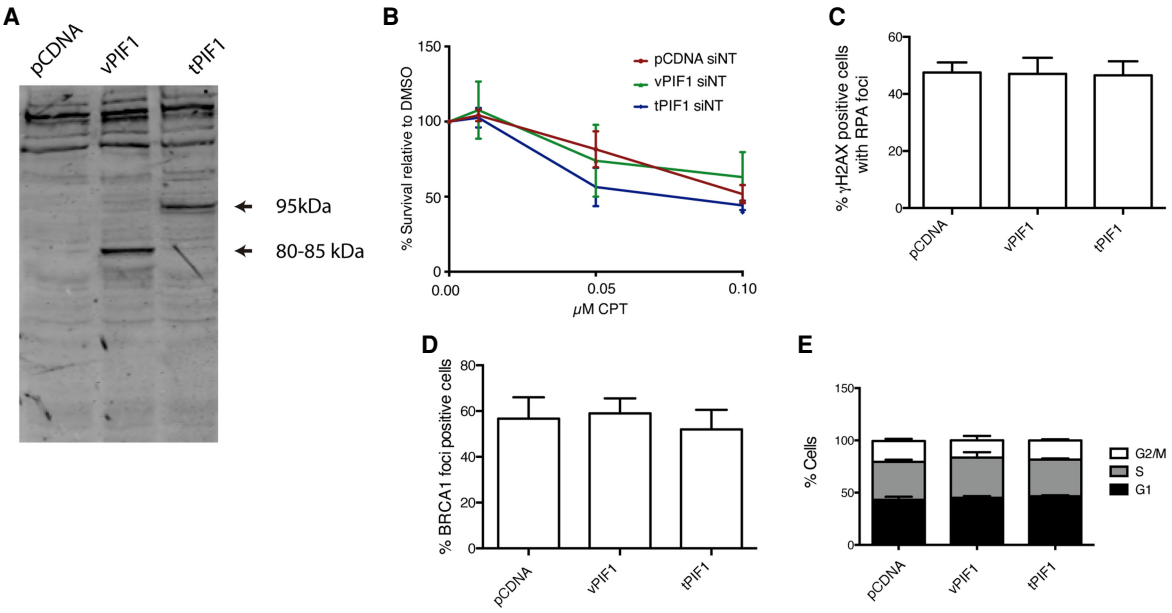

FIGURE 5. Expression of different PIF1 splicing variants. (*A*) Western blot showing the abundance of different PIF1 isoforms in cells transfected with the empty pCDNA plasmid or pCDNA bearing the vPIF1 or tPIF1 splicing variants. (*B*) Percentage of survival to different doses of camptothecin (CPT) in cells overexpressing the tPIF1 or vPIF1 isoforms relative to the DMSO treated control, as indicated. Cells transfected with the empty pCDNA vector were used as a control. The average and standard deviations of three independent experiments are shown. (*C*) Percentage of cells positive for RPA foci upon exposure to 10 Gy of ionizing radiation. Cells expressed the indicated PIF1 variants. An empty pCDNA vector was used as a control. The average and standard deviations of three independent experiments are shown. No statistically significant differences were found using an ANOVA test. (*D*) Same as *A*, but for BRCA1 foci. (*E*) Cell cycle analysis of cells transfected with the indicated plasmids. The percentage of cells in each cell cycle phase was analyzed as described in the Materials and Methods section. The average and standard deviation of three independent experiments is shown.

splicing of key DDR factors, such as *BRCA1*, *RAD51*, *RIF1*, *DNA2*, and *EXO1*. This might reflect a critical role of the SF3B complex in preparing the cells for the exposure to genotoxic agents.

Similarly, we show that CtIP affects the mRNA accumulation of hundreds of transcripts. This agrees, in principle, with the established role of CtIP in transcription (Li et al. 1999; Koipally and Georgopoulos 2002; Sum et al. 2002; Liu and Lee 2006; Xu et al. 2007; Liao et al. 2010; Liu et al. 2014). However, we also observe a prominent effect in splicing genome-wide. Such a role seems to require the functional interaction with the SF3B complex, as the majority of those events were altered also when SF3B2 was depleted. Splicing occurs cotranscriptionally and there is an intense crosstalk between transcription efficiency and splicing (Howe et al. 2003; Ip et al. 2011; Braunschweig et al. 2014; Fong et al. 2014; Aslanzadeh et al. 2018). Thus, transcription impairment could modify splicing efficiency and, on the contrary and as discussed for SF3B above, defective splicing might affect accumulation of mRNA that can be, erroneously, interpreted as transcriptional defects. So, in the case of CtIP it is not so clear if

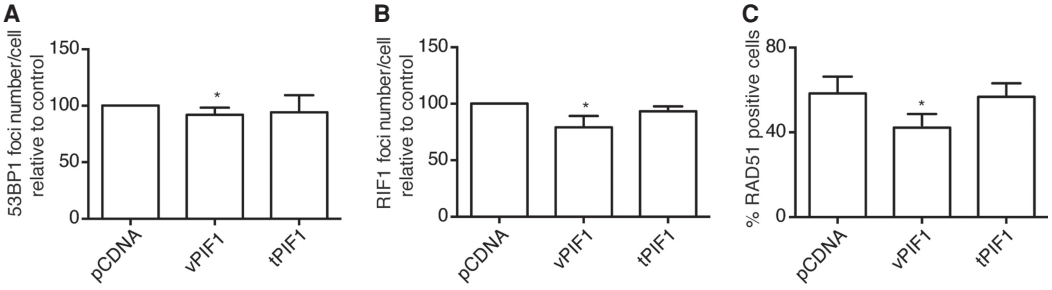

FIGURE 6. PIF1 splicing variants affect the recruitment of DDR factors. (*A*) Average number of 53BP1 foci per cell upon exposure to 10 Gy of IR in cells transfected with the indicated vectors relative to control cells. The average and standard deviation of three independent experiments is shown. Statistical significance was calculated using an ANOVA test. (*) $P < 0.05$. (*B*) Same as *A* but for RIF1 foci. (*C*) Same as *A* but for RAD51 foci.

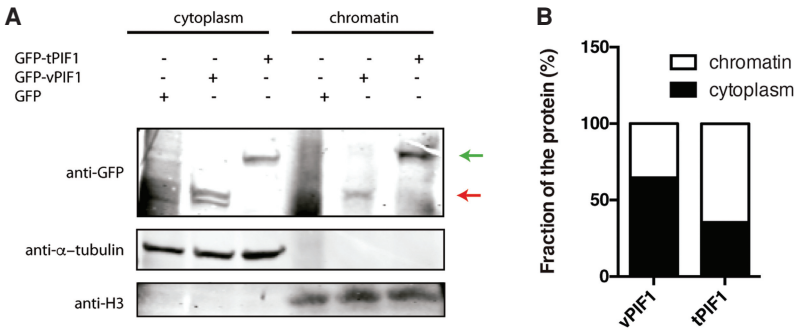

FIGURE 7. Cellular localization of PIF1 splicing variants. (*A*) Protein samples from undamaged cells expressing the indicated PIF1 isoforms were fractionated as described in the Materials and Methods section. Cytoplasmic and chromatin fractions were resolved in SDS-PAGE and blotted with the indicated antibodies. vPIF1 is marked with a red arrow. tPIF1 is located with a green arrow. A representative experiment is shown. (*B*) Western blots from *A* were quantified using an Odyssey Infrared Imaging System (LI-COR) and ImageStudio software (LI-COR). The ration between the cytoplasmic and chromatin fraction of each PIF1 isoform is represented.

those two roles, in transcription and splicing, are really two independent functions or simply both sides of the same coin. In any case, the regulation of the accumulation of different species of mRNA of many genes might explain why CtIP seems to play so many different roles in many processes. Indeed, there is evidence of other cases in which a RNA metabolism protein modulates its role in DDR through regulating the splicing of other factors involved in that process (Savage et al. 2014; Shkreta and Chabot 2015; Pederiva et al. 2016). For example, PRMT5 regulates its effects on DNA repair by controlling the RNA splicing of several epigenetic regulators, especially the histone H4 acetyl-transferase TIP60 (KAT5) and the histone H4 methyltransferase SUV4-20H2 (KMT5C) (Hamard et al. 2018).

We propose that, for many phenotypes, and especially including DNA end resection, recombination, and the DNA damage response, CtIP and SF3B probably participate at two different levels, directly, working as repair factors (Prados-Carvajal et al. 2018), but also indirectly as general transcription/splicing regulators. In that regard, they closely resemble its interactor BRCA1, which also seems to be involved at many different levels. Such double involvement of some RNA factors in DNA repair, which has simultaneous RNA-mediated and RNA-indirect roles in homologous recombination, was also observed by other authors (Anantha et al. 2013). This creates complex regulatory networks that are able to integrate multiple cellular signals and elicit sophisticated responses that fine-tune the response.

Other proteins are likely involved in such complex networks, including the helicase PIF1. Interestingly, PIF1 and CtIP directly interacts and participates in resection of DSBs at atypical DNA structures such as G-quadruplexes (Jimeno et al. 2018b). But additionally, we have shown here that CtIP controls a DNA damage alternative splicing of PIF1 that modulates the response to DNA damaging agents. A proficient DDR seems to require a timely switch between the two forms described here, the tPIF1 and vPIF1. Whereas vPIF1 slightly impairs early events in DNA repair, its presence ensures a better survival to DNA damage. On the contrary, the presence of tPIF1 does not affect those early events, but if maintained in time compromise viability of cells exposed to camptothecin. Interestingly, the main difference between both forms is the change in cellular localization and the presence of an active helicase domain. Whereas tPIF1 maintains such activity, vPIF1 lacks exon 9 and, therefore, misses part of the active site. Thus, it is likely that tPIF1 participates on DNA end resection and DNA repair early on, working on a DNA substrate as a helicase. However, our data suggest that

TABLE 8. shRNAs and siRNAs used

Target gene	Reference	Supplier	Sequence (5′–3′)
Nontarget	D-001810-10-20	Dharmacon	UGGUUUACAUGUCGACUAA, UGGUUUACAUGUUGUGUGA, UGGUUUACAUGUUUUCUGA and UGGUUUACAUGUUUUCCUA (mix)
CtIP	Huertas and Jackson (2009)	Sigma	GCUAAAACAGGAACGAAUC
SF3B2	HSC.RNAI.N006843.12.6	IDT	GGACUUGUCAUUUCAUGUUCUUATT
PIF1	N/A	IDT	GGAUGUUCUCAGGUUGUAUUUAUTT
pLKO.1-shNT	SHC016V	Sigma	CCGGGGCGCGATAGCGCTAATAATTTCTCGAGAAATTATTAGCGCTATCGCGCTTTTT
pLKO.1-shCtIP	NM_002894.1-3008s1c1	Sigma	CCGGCAGAAGGATGAAGGACAGTTTCTCGAGAAACTGTCCTTCATCCTTCTGTTTTT
pLKO.1-shSF3B2	NM_006842.2-1133s21c1	Sigma	CCGGGCTGATGTTGAGATTGAGTATCTCGAGATACTCAATCTCAACATCAGCTTTTTG

TABLE 9. Primary antibodies used in this study

Target protein	Source	Supplier/reference	Application	Dilution
GFP	Rabbit	Santa Cruz (sc-8334)	WB	1:1000
α-tubulin	Mouse	Sigma (T9026)	WB	1:50000
β-actin	Rabbit	Abcam (ab8227)	WB	1:50000
RPA32	Mouse	Abcam (ab2175)	IF	1:500
γH2AX	Rabbit	Cell signaling (2577L)	IF	1:500
RAD51	Mouse	Abcam; ab213	IF	1:1000
BRCA1	Mouse	Santa Cruz (sc-6954)	WB, IF	1:1000, 1:200
53BP1	Rabbit	NB100-304, Novus	WB, IF	1:1000, 1:500
RIF1	Mouse	Bethyl Laboratories (A300-568A)	WB, IF	1:500, 1:200
CtIP	Mouse	R. Baer (14.1)	WB	1:500
SF3B2	Rabbit	Proteintech (10919-1-AP)	WB	1:1000
PIF1	Mouse	Santa Cruz (sc-48377)	WB	1:500

WB, western blotting. IF, immunofluorescence.

cells prefer to reduce this active PIF1 pool to ensure survival. One possibility is that the switch between both isoforms reduces the active pool of the helicase, both by sending the protein to the cytoplasm and by destroying the active site, to avoid interference of the helicase with very late steps of DNA repair or the DDR. Alternatively, it is formally possible that the vPIF1 plays some active role in the cytoplasm that facilitates survival. Considering that another isoform, PIF1β is essential for mitochondrial metabolism, we could not exclude this hypothetical function, although it will imply a role that does not require a functional helicase domain. In any case, PIF1 alternative splicing illustrates how CtIP might have additional effects in the response to DNA damage that has been, so far, overlooked. Strikingly, our data suggest that the regulation of PIF1 is modulated by the threonine 847 of CtIP, although not because resection is impaired by this mutant. This residue is a well established CDK site (Huertas 2010; Polato et al. 2014). Interestingly, and albeit less clearly, CDK phosphorylation of CtIP S327 seems also involved. Hence, it is possible that upon DNA damage but only in cells in the G1 phase of the cell cycle, CtIP activates the expression of the isoform called vPIF1. This will separate the different roles of CtIP in a cell cycle dependent manner, with the DNA damage-induced splicing function mainly on G1 and the DNA end resection and homologous recombination exclusively in S and G2. Similar differential roles to maintain genome stability during the cell cycle have been reported for other factors before. For example, Rad^{4TopBP1} selectively activates checkpoint responses to DNA damage or replication perturbation depending on the cell cycle (Taricani and Wang 2006).

In agreement with a tight relationship between BRCA1, CtIP and the SF3B complex, all three are intimately related to cancer appearance and, more specifically, with breast cancer incidence (Soria-Bretones et al. 2013; Paul and Paul 2014; Maguire et al. 2015; Gokmen-Polar et al. 2019). In the case of CtIP and BRCA1, this connection with cancer has been mostly explained as a defective DNA repair. However, considering the involvement of CtIP, described here, and BRCA1 (Savage et al. 2014) in RNA splicing, maybe the cancer connection should be revisited in light of those novel roles. Conversely, recent studies have detected recurrent mutations in components of the spliceosome in myelodysplastic syndromes (Shiozawa et al. 2018; Pollyea et al. 2019), renal cell carcinoma

TABLE 10. Secondary antibodies used in this study

Antibody	Supplier/reference	Application	Dilution
IRDye 680RD goat anti-mouse IgG (H + L)	LI-COR (926-68070)	WB	1:10000
IRDye 800CW goat anti-rabbit IgG (H + L)	LI-COR (926-32211)	WB	1:10000
Alexa Fluor 594 goat anti-mouse	Invitrogen (A11032)	IF	1:1000
Alexa Fluor 488 goat anti-rabbit	Invitrogen (A11034)	IF	1:1000

WB, western blotting. IF, immunofluorescence.

(Yang et al. 2017; Verma and Das 2018), chronic lymphocytic leukemia (Agrawal et al. 2017; Maleki et al. 2019), lung adenocarcinoma (Kim et al. 2018; Mao et al. 2019), breast cancer (Gokmen-Polar et al. 2019; Zhao et al. 2019), or pancreatic cancer (Tian et al. 2015; Zhou et al. 2017). Moreover, alterations in expression of splicing factors, including SF3B, can derive in various types of cancers (Goswami et al. 2014; Maguire et al. 2015; Alsafadi et al. 2016; Zheng et al. 2018). This probably reflects the importance of mRNA splice variants of several significant genes in apoptosis, metabolism, and angiogenesis (Grosso et al. 2008). However, another tantalizing possibility, not yet analyzed in detail, is that some of those connections of SF3B with cancer might be a consequence of its more direct role in DNA repair. Furthermore, it might be possible to exploit the defective DNA repair and DDR in SF3B deficient cancer for therapeutic interventions. Thus, this crosstalk between DNA repair and the DDR and splicing might become in the future an important target for cancer treatment.

MATERIALS AND METHODS

Cell lines and growth conditions

U2OS human cell lines were grown in DMEM (Sigma-Aldrich) supplemented with 10% fetal bovine serum (Sigma-Aldrich), 2 mM L-glutamine (Sigma-Aldrich) and 100 units/mL penicillin and 100 µg/mL streptomycin (Sigma-Aldrich). For cells expressing GFP-tPIF1 and GFP-vPIF1, medium was supplemented with 0.5 mg/mL G418 (Sigma).

shRNAs, siRNAs, plasmids, and transfections

shRNAs and siRNA duplexes were obtained from Sigma-Aldrich, Dharmacon, or Qiagen (Table 8) and were transfected using RNAiMax Lipofectamine Reagent Mix (Life Technologies), according to the manufacturer's instructions. Plasmid transfection of U2OS cells with PIF1 variants was carried out using FuGENE 6 Transfection Reagent (Promega) according to the manufacturer's protocol.

To generate the lentivirus harboring the shRNA, HEK293T cells were transfected with the plasmids containing the specific shRNA (pLKO.1), p8.91 and pVSVG in a ratio 3:2:1. The DNA mix was prepared in a volume of 1 mL containing 250 mM CaCl2 and was added dropwise while bubbling into 1 mL of 2× HEPES buffered saline (Sigma). The mix was incubated 30 min at room temperature and added dropwise to the cells while carefully rocking the plate. Two days after transfection, medium was collected and filtered using 0.45 µm polyvinylidene difluoride (PVDF) filters (Millipore) and 8 µg/mL polybrene (Sigma,) was added. For transduction, cells were seeded, and 24 h later medium with lentiviruses was thawed and added to the plates. The medium was replaced 8 h later to remove viral residues and polybrene. Knockdowns were validated by western blot 48 h after transduction.

Cell fractionation

U2OS cells stably expressing the different PIF1 isoforms were subjected to nuclear/cytoplasm fractionation to analyze the distribution of both PIF1 variants in the different cellular compartments basically following the protocol described by Philpott and colleagues (Gillotin et al. 2018). Briefly, after washing the cells once with room temperature PBS, they were resuspended into 1 mL PBS and then pelleted at 1200 rpm at 4°C for 3 min. Pellets were covered with 5 volumes of ice-cold E1 buffer (50 mM Hepes-KOH pH 7.5, 140 mM NaCl, 1 mM EDTA pH 8.0, 10% glycerol, 0.5% NP-40, 0.25% triton X-100, 1 mM DTT) complemented with 1× protease inhibitor cocktail and gently pipetted up and down (five times). After centrifugation at 3400 rpm at 4°C for 2 min, the supernatant was collected (cytoplasmic fraction). Then the pellet was washed in the same volume of E1 buffer. The pellet was resuspended in the same volume of E1 and incubated for 10 min on ice. Upon centrifugation at 3400 rpm at 4°C for 2 min, the supernatant was discarded. The pellet was resuspended by gentle pipetting in two volumes of ice-cold E2 buffer (10 mM Tris-HCl pH8.0, 200 mM NaCl, 1 mM EDTA pH 8.0, 0.5 mM EGTA pH8.0) complemented with 1× protease inhibitor cocktail and then centrifuged at 3400 rpm at 4°C for 2 min. The supernatant was collected in a fresh tube (nucleus fraction). The pellet was washed in the same volume of E2, resuspended in the same volume of E2 and incubated for 10 min on ice. Upon centrifugation at 3400 rpm at 4°C for 2 min, the supernatant was discarded, and the pellet was resuspended in ice-cold E3 buffer (500 mM Tris-HCl, 500 mM NaCl) complemented with 1× protease inhibitor cocktail. The solution (chromatin fraction) was sonicated to solubilize the proteins. All fractions were then centrifuged at 13,000 rpm at 4°C for 10 min to clarify the solution.

SDS-PAGE and western blot analysis

Protein extracts were prepared in 2× Laemmli buffer (4% SDS, 20% glycerol, 125 mM Tris-HCl, pH 6.8) and passed 10 times through a 0.5 mm needle-mounted syringe to reduce viscosity. Proteins were resolved by SDS-PAGE and transferred to low fluorescence PVDF membranes (Immobilon-FL, Millipore). Membranes were blocked with Odyssey Blocking Buffer (LI-COR) and blotted with the appropriate primary antibody (Table 9) and infrared dyed secondary antibodies (LI-COR) (Table 10). Antibodies were prepared in Blocking Buffer supplemented with 0.1% Tween-20. Membranes were air-dried in the dark and scanned in an Odyssey Infrared Imaging System (LI-COR), and images were analyzed with ImageStudio software (LI-COR).

Immunofluorescence and microscopy

For RPA foci visualization, U2OS cells knocked down for different proteins were seeded on coverslips. At 1 h after either irradiation (10 Gy), coverslips were washed once with PBS followed by treatment with Preextraction Buffer (25 mM Tris-HCl, pH 7.5, 50 mM NaCl, 1 mM EDTA, 3 mM MgCl2, 300 mM sucrose and 0.2% Triton X-100) for 5 min on ice. To visualize RAD51 foci, cells were cultured for 3 h after irradiation. To visualize BRCA1 foci, Preextraction Buffer 2 (10 mM PIPES pH 6.8, 300 mM sucrose, 50mM NaCl, 3mM EDTA, 25× proteinase inhibitor and 0.5%

Triton X-100) was used. Cells were fixed with 4% paraformaldehyde (w/v) in PBS for 15 min. Following two washes with PBS, cells were blocked for 1 h with 5% FBS in PBS, costained with the appropriate primary antibodies (Table 9) in blocking solution overnight at 4°C or for 2 h at room temperature, washed again with PBS and then coimmunostained with the appropriate secondary antibodies for 1 h (Table 10) in Blocking Buffer. After washing with PBS and drying with ethanol 70% and 100% washes, coverslips were mounted into glass slides using Vectashield mounting medium with DAPI (Vector Laboratories). RPA foci immunofluorescences were analyzed using a Leica Fluorescence microscope.

For 53BP1 visualization, U2OS cells were seeded and transfected as previously described. Once collected, cells were fixed with methanol (VWR) for 10 min on ice, followed by treatment with acetone (Sigma) for 30 sec on ice. For RIF1 foci visualization, cells were fixed with 4% PFA for 15 min, washed twice with 1× PBS and then permeabilized for 15 min with 0.25% Triton diluted in 1× PBS. Samples were immunostained as described above with the appropriate primary and secondary antibodies (Tables 9, 10). Images obtained with a Leica Fluorescence microscope were then analyzed using Metamorph to count the number of foci per cell.

Cell cycle analysis

Cells were fixed with cold 70% ethanol overnight, incubated with 250 µg/mL RNase A (Sigma) and 10 µg/mL propidium iodide (Fluka) at 37°C for 30 min. For each replicate, 10,000 cells were analyzed with a FACSCalibur (BD). Cell cycle distribution data were further analyzed using ModFit LT 3.0 software (Verity Software House, Inc).

RNA extraction, reverse transcription, and quantitative PCR

RNA extracts were obtained from cells using NZY Total RNA Isolation kit (Nzytech) according to manufacturer's instructions. To obtain complementary DNA (cDNA), 1 µg RNA was subjected to RQ1 DNase treatment (Promega) prior to reverse transcription reaction using Maxima H Minus First Strand cDNA Synthesis kit (Thermo Scientific) according to manufacturer's instructions. Quantitative PCR from cDNA was performed to check siRNA-mediated knockdown of several proteins. For this, iTaq Universal SYBR Green Supermix (Bio-Rad) was used following manufacturer's instructions. DNA primers used for qPCR are listed in Table 4. Q-PCR was performed in an Applied Biosystem 7500 FAST Real-Time PCR system. The comparative threshold cycle (C_t) method was used to determine relative transcript levels (Bulletin 5279, Real-Time PCR Applications Guide, Bio-Rad), using β-actin expression as internal control. Expression levels relative to β-actin were determined with the formula $2^{-\Delta\Delta Ct}$ (Livak and Schmittgen 2001). To analyze *PIF1* exon junctions, the data were also normalized to an exon constitutively expressed in the cell.

Microarray

To analyze RNA splicing genome-wide from cells depleted or not for SF3B2 or CtIP in damaged (10 Gy) and untreated conditions the splicing microarray Transcriptome Arrays HTA & MTA (Affymetrix) were used as previously described (Jimeno-González et al. 2015). This array design contains >6.0 million distinct probes covering coding and noncoding transcripts. 70% of the probes cover exons for coding transcripts, and 30% of probes on the array cover exon–exon splice junctions and noncoding transcripts. The array contains approximately 10 probes per exon and four probes per exon–exon splice junction. RNA was obtained using an RNA isolation kit, as explained in the section above, in triplicates. The purity and quality of isolated RNA were assessed by RNA 6000 Nano assay on a 2100 Bioanalyzer (Agilent Technologies). Total RNA from each sample (250 ng) was used to generate amplified and biotinylated sense-strand cDNA from the entire expressed genome according to the GeneChip WT PLUS Reagent Kit User Manual (P/N 703174 Rev 1; Affymetrix, Inc.). GeneChip HTA Arrays were hybridized for 16 h in a 45°C oven, rotated at 60 rpm. According to the GeneChip Expression Wash, Stain and Scan Manual (PN 702731 Rev 3; Affymetrix, Inc.), the arrays were washed and stained using the Fluidics Station 450 and finally were scanned using the GeneChip Scanner 3000 7G. Raw data were extracted from the scanned images and analyzed with the Affymetrix Command Console 2.0 Software. The raw array data were preprocessed and normalized using the Robust Multichip Average method. Data were processed further using Transcriptome Analysis Console (TAC) Software from Affymetrix, which performs a gene-level analysis or an alternative splicing analysis. For gene-level analysis, gene expression changes with $P < 0.05$ (ANOVA) and a linear fold change$| \geq 2$ were considered significant. For alternative splicing analysis, the splicing index (SI) was calculated as SI = Log_2[(Probe – set1Doxintensity/Gene1Doxintensity)/(Probe – set1ControlIntensity/Gene1ControlIntensity)]. Splicing changes were considered significant when the |splicing index| was ≥2 and $P < 0.05$ (ANOVA).

Array data also were analyzed using AltAnalyze software (Emig et al. 2010) version 2.0 with core probe set filtering using DABG (detected above background; *P*-value cutoff of 0.05) and microarray analysis of differential splicing (MiDAS exon analysis parameters; *P*-value cutoff of 0.05). The signs of the splicing index values obtained from AltAnalyze were changed to use the same splicing index definition throughout the manuscript. AltAnalyze incorporates a library of splicing annotations from UCSC KnownAlt database. GeneChip HTA 2.0 arrays include probes to detect 245.349 different transcript variants, supported by a variable number of ESTs in the databases. Intronic regions often are represented in the ESTs databases because of the retrotranscription of unspliced pre-mRNAs, aberrant splicing forms, and spurious firing of cryptic promoters inside introns, with functional or nonfunctional implications. For that reason, GeneChip HTA 2.0 arrays allow the identification of an intron-retention event (media.affymetrix.com/support/technical/datasheets/hta_array_2_0_datasheet.pdf).

Statistical analysis

Statistical significance was determined with a Student's *t*-test or ANOVA as indicated using PRISM software (Graphpad Software, Inc.). Statistically significant differences were labeled with one, two or three asterisks for $P < 0.05$, $P < 0.01$, or $P < 0.001$, respectively.

SUPPLEMENTAL MATERIAL

Supplemental material is available for this article.

ACKNOWLEDGMENTS

We wish to thank Jose Carlos Reyes for critical reading of the manuscript. This work was financed by an R+D+I grant from the Spanish Ministry of Economy and Competitivity (SAF2016-74855-P) and by the European Union Regional Funds (FEDER). R.P.-C. was funded with an FPU fellowship from the Spanish Ministry of Education, and G.R.-R. was supported by the Regional Government of Andalucía (Junta de Andalucía) with a contract of the program "Garantía juvenil en la Universidad de Sevilla." CABIMER is supported by the regional government of Andalucía (Junta de Andalucía).

Received November 26, 2020; accepted December 4, 2020.

REFERENCES

Adamson B, Smogorzewska A, Sigoillot FD, King RW, Elledge SJ. 2012. A genome-wide homologous recombination screen identifies the RNA-binding protein RBMX as a component of the DNA-damage response. *Nat Cell Biol* **14:** 318–328. doi:10.1038/ncb2426

Agrawal AA, Seiler M, Brinton LT, Mantel R, Lapalombella R, Woyach JA, Johnson AJ, Zhu P, Warmuth M, Yu L, et al. 2017. Novel SF3B1 in-frame deletions result in aberrant RNA splicing in CLL patients. *Blood Adv* **1:** 995–1000. doi:10.1182/bloodadvances.2017007062

Alsafadi S, Houy A, Battistella A, Popova T, Wassef M, Henry E, Tirode F, Constantinou A, Piperno-Neumann S, Roman-Roman S, et al. 2016. Cancer-associated SF3B1 mutations affect alternative splicing by promoting alternative branchpoint usage. *Nat Commun* **7:** 10615. doi:10.1038/ncomms10615

Anantha RW, Alcivar AL, Ma J, Cai H, Simhadri S, Ule J, Konig J, Xia B. 2013. Requirement of heterogeneous nuclear ribonucleoprotein C for BRCA gene expression and homologous recombination. *PLoS One* **8:** e61368. doi:10.1371/journal.pone.0061368

Aslanzadeh V, Huang Y, Sanguinetti G, Beggs JD. 2018. Transcription rate strongly affects splicing fidelity and cotranscriptionality in budding yeast. *Genome Res* **28:** 203–213. doi:10.1101/gr.225615.117

Barbier J, Dutertre M, Bittencourt D, Sanchez G, Gratadou L, de la Grange P, Auboeuf D. 2007. Regulation of H-ras splice variant expression by cross talk between the p53 and nonsense-mediated mRNA decay pathways. *Mol Cell Biol* **27:** 7315–7333. doi:10.1128/MCB.00272-07

Beli P, Lukashchuk N, Wagner SA, Weinert BT, Olsen JV, Baskcomb L, Mann M, Jackson SP, Choudhary C. 2012. Proteomic investigations reveal a role for RNA processing factor THRAP3 in the DNA damage response. *Mol Cell* **46:** 212–225. doi:10.1016/j.molcel.2012.01.026

Bennetzen MV, Larsen DH, Bunkenborg J, Bartek J, Lukas J, Andersen JS. 2010. Site-specific phosphorylation dynamics of the nuclear proteome during the DNA damage response. *Mol Cell Proteomics* **9:** 1314–1323. doi:10.1074/mcp.M900616-MCP200

Boucas J, Riabinska A, Jokic M, Herter-Sprie GS, Chen S, Höpker K, Reinhardt HC. 2012. Posttranscriptional regulation of gene expression-adding another layer of complexity to the DNA damage response. *Front Genet* **3:** 159. doi:10.3389/fgene.2012.00159

Braunschweig U, Barbosa-morais NL, Pan Q, Nachman EN, Alipanahi B, Gonatopoulos-pournatzis T, Frey B, Irimia M, Blencowe BJ. 2014. Widespread intron retention in mammals functionally tunes transcriptomes. *Genome Res* **24:** 1774–1786. doi:10.1101/gr.177790.114

Ciccia A, Elledge SJ. 2010. The DNA damage response: making it safe to play with knives. *Mol Cell* **40:** 179–204. doi:10.1016/j.molcel.2010.09.019

Cloutier A, Shkreta L, Toutant J, Durand M, Thibault P, Chabot B. 2018. HnRNP A1/A2 and Sam68 collaborate with SRSF10 to control the alternative splicing response to oxaliplatin-mediated DNA damage. *Sci Rep* **8:** 1–14. doi:10.1038/s41598-018-20360-x

Cruz-García A, López-Saavedra A, Huertas P. 2014. BRCA1 accelerates CtIP-mediated DNA-end resection. *Cell Rep* **9:** 451–459. doi:10.1016/j.celrep.2014.08.076

D'Alessandro G, Whelan DR, Howard SM, Vitelli V, Renaudin X, Adamowicz M, Iannelli F, Jones-Weinert CW, Lee MY, Matti V, et al. 2018. BRCA2 controls DNA:RNA hybrid level at DSBs by mediating RNase H2 recruitment. *Nat Commun* **9:** 5376. doi:10.1038/s41467-018-07799-2

Duquette ML, Zhu Q, Taylor ER, Tsay AJ, Shi LZ, Berns MW, McGowan CH. 2012. CtIP is required to initiate replication-dependent interstrand crosslink repair. *PLoS Genet* **8:** 26–28. doi:10.1371/journal.pgen.1003050

Elia AEH, Boardman AP, Wang DC, Huttlin EL, Everley RA, Dephoure N, Zhou C, Koren I, Gygi SP, Elledge SJ. 2015. Quantitative proteomic atlas of ubiquitination and acetylation in the DNA damage response. *Mol Cell* **59:** 867–881. doi:10.1016/j.molcel.2015.05.006

Emig D, Salomonis N, Baumbach J, Lengauer T, Conklin BR, Albrecht M. 2010. AltAnalyze and domainGraph: analyzing and visualizing exon expression data. *Nucleic Acids Res* **38:** 755–762. doi:10.1093/nar/gkq405

Fan J, Yang X, Wang W, Wood WH, Becker KG, Gorospe M. 2002. Global analysis of stress-regulated mRNA turnover by using cDNA arrays. *Proc Natl Acad Sci* **99:** 10611–10616. doi:10.1073/pnas.162212399

Fong N, Kim H, Zhou Y, Ji X, Qiu J, Saldi T, Diener K, Jones K, Fu XD, Bentley DL. 2014. Pre-mRNA splicing is facilitated by an optimal RNA polymerase II elongation rate. *Genes Dev* **28:** 2663–2676. doi:10.1101/gad.252106.114

Futami K, Shimamoto A, Furuichi Y. 2007. Mitochondrial and nuclear localization of human Pif1 helicase. *Biol Pharm Bull* **30:** 1685–1692. doi:10.1248/bpb.30.1685

Gasch AP, Huang M, Metzner S, Botstein D, Elledge SJ, Brown PO. 2001. Genomic expression responses to DNA-damaging agents and the regulatory role of the yeast ATR homolog Mec1p. *Mol Biol Cell* **12:** 2987–3003. doi:10.1091/mbc.12.10.2987

Gillotin S, Davies JD, Philpott A. 2018. Subcellular localisation modulates ubiquitylation and degradation of Ascl1. *Sci Rep* **8:** 1–13. doi:10.1038/s41598-018-23056-4

Gokmen-Polar Y, Neelamraju Y, Goswami CP, Gu Y, Gu X, Nallamothu G, Vieth E, Janga SC, Ryan M, Badve SS. 2019. Splicing factor ESRP1 controls ER-positive breast cancer by altering metabolic pathways. *EMBO Rep* **20:** e46078. doi:10.15252/embr.201846078

Golas MM, Sander B, Will CL, Luhrmann R, Stark H. 2003. Molecular architecture of the multiprotein splicing factor SF3b. *Science* **300:** 980–984. doi:10.1126/science.1084155

Goswami CP, Janga SC, Gu X, Nallamothu G, Neelamraju Y, Gökmen-Polar Y, Badve S. 2014. Expression levels of SF3B3 correlate with prognosis and endocrine resistance in estrogen receptor-positive breast cancer. *Mod Pathol* **28:** 677–685.

Grosso AR, Martins S, Carmo-Fonseca M. 2008. The emerging role of splicing factors in cancer. *EMBO Rep* **9:** 1087–1093. doi:10.1038/embor.2008.189

Hamard P, Santiago GE, Liu F, Greenblatt S, Verdun RE, Nimer SD, Hamard P, Santiago GE, Liu F, Karl DL, et al. 2018. PRMT5 regulates DNA repair by controlling the alternative splicing of histone-modifying enzymes article PRMT5 regulates DNA repair by controlling the alternative splicing of histone-modifying enzymes. *Cell Rep* **24:** 2643–2657. doi:10.1016/j.celrep.2018.08.002

Howe KJ, Kane CM, Ares M. 2003. Perturbation of transcription elongation influences the fidelity of internal exon inclusion in *Saccharomyces cerevisiae*. *RNA* **9:** 993–1006. doi:10.1261/rna.5390803

Huertas P. 2010. DNA resection in eukaryotes: deciding how to fix the break. *Nat Struct Mol Biol* **17:** 11–16. doi:10.1038/nsmb.1710

Huertas P, Jackson SP. 2009. Human CtIP mediates cell cycle control of DNA end resection and double strand break repair. *J Biol Chem* **284:** 9558–9565. doi:10.1074/jbc.M808906200

Ip J, Schmidt D, Pan Q. 2011. Global impact of RNA polymerase II elongation inhibition on alternative splicing regulation. *Genome Res* **21:** 390–401. doi:10.1101/gr.111070.110

Jackson SP, Bartek J. 2009. The DNA-damage response in human biology and disease. *Nature* **461:** 1071–1078. doi:10.1038/nature08467

Jasin M, Rothstein R. 2013. Repair of strand breaks by homologous recombination. *Cold Spring Harb Perspect Biol* **5:** a012740. doi:10.1101/cshperspect.a012740

Jimeno S, Camarillo R, Mejias-Navarro F, Fernandez-Avila MJ, Soria-Bretones I, Prados-Carvajal R, Huertas P. 2018a. The helicase PIF1 facilitates resection over sequences prone to forming G4 structures. *Cell Rep* **24:** 3262–3273.e4. doi:10.1016/j.celrep.2018.08.047

Jimeno S, Camarillo R, Mejías-Navarro F, Fernández-Ávila MJ, Soria-Bretones I, Prados-Carvajal R, Huertas P. 2018b. The helicase PIF1 facilitates resection over sequences prone to forming G4 structures. *Cell Rep* **24:** 3262–3273. doi:10.1016/j.celrep.2018.08.047

Jimeno S, Prados-Carvajal R, Huertas P. 2019. The role of RNA and RNA-related proteins in the regulation of DNA double strand break repair pathway choice. *DNA Repair (Amst)* **81:** 102662. doi:10.1016/j.dnarep.2019.102662

Jimeno-González S, Payán-Bravo L, Muñoz-Cabello AM, Guijo M, Gutierrez G, Prado F, Reyes JC. 2015. Defective histone supply causes changes in RNA polymerase II elongation rate and cotranscriptional pre-mRNA splicing. *Proc Natl Acad Sci* **112:** 14840–14845. doi:10.1073/pnas.1506760112

Kim S, Park C, Jun Y, Lee S, Jung Y, Kim J. 2018. Integrative profiling of alternative splicing induced by U2AF1 S34F mutation in lung adenocarcinoma reveals a mechanistic link to mitotic stress. *Mol Cells* **41:** 733–741.

Kleiman FE, Wu-Baer F, Fonseca D, Kaneko S, Baer R, Manley JL. 2005. BRCA1/BARD1 inhibition of mRNA 3′ processing involves targeted degradation of RNA polymerase II. *Genes Dev* **19:** 1227–1237. doi:10.1101/gad.1309505

Koipally J, Georgopoulos K. 2002. Ikaros-CtIP interactions do not require C-terminal binding protein and participate in a deacetylase-independent mode of repression. *J Biol Chem* **277:** 23143–23149. doi:10.1074/jbc.M202079200

Li S, Chen PL, Subramanian T, Chinnadurai G, Tomlinson G, Osborne CK, Sharp ZD, Lee WH. 1999. Binding of CtIP to the BRCT repeats of BRCA1 involved in the transcription regulation of p21 is disrupted upon DNA damage. *J Biol Chem* **274:** 11334–11338. doi:10.1074/jbc.274.16.11334

Liao C-C, Tsai CY, Chang W-C, Lee W-H, Wang J-M. 2010. RB.E2F1 complex mediates DNA damage responses through transcriptional regulation of ZBRK1. *J Biol Chem* **285:** 33134–33143. doi:10.1074/jbc.M110.143461

Lieber MR. 2010. The mechanism of double-strand DNA break repair by the nonhomologous DNA end-joining pathway. *Annu Rev Biochem* **79:** 181–211. doi:10.1146/annurev.biochem.052308.093131

Liu F, Lee W. 2006. CtIP activates its own and Cyclin D1 promoters via the E2F/RB pathway during G_1/S progression. *Mol Cell Biol* **26:** 3124–3134. doi:10.1128/MCB.26.8.3124-3134.2006

Liu B, Cong R, Peng B, Zhu B, Dou G, Ai H, Zhang X, Wang Z, Xu X. 2014. CtIP is required for DNA damage-dependent induction of P21. *Cell Cycle* **13:** 90–95. doi:10.4161/cc.26810

Livak KJ, Schmittgen TD. 2001. Analysis of relative gene expression data using real-time quantitative PCR and the $2^{-\Delta\Delta C_T}$ method. *Methods* **25:** 402–408. doi:10.1006/meth.2001.1262

Maguire SL, Leonidou A, Wai P, Marchiò C, Ng CKY, Sapino A, Salomon A, Reis-filho JS, Weigelt B, Natrajan RC. 2015. SF3B1 mutations constitute a novel therapeutic target in breast cancer. *J Pathol* 571–580. doi:10.1002/path.4483

Makharashvili N, Paull TT. 2015. CtIP: a DNA damage response protein at the intersection of DNA metabolism. *DNA Repair (Amst)* **32:** 75–81. doi:10.1016/j.dnarep.2015.04.016

Makharashvili N, Arora S, Yin Y, Fu Q, Wen X, Lee J-H, Kao C-H, Leung JW, Miller KM, Paull TT. 2018. Sae2/CtIP prevents R-loop accumulation in eukaryotic cells. *Elife* **7:** 1–33. doi:10.7554/eLife.42733

Maleki Y, Alahbakhshi Z, Heidari Z, Moradi M-T, Rahimi Z, Yari K, Rahimi Z, Aznab M, Ahmadi-Khajevand M, Bahremand F. 2019. NOTCH1, SF3B1, MDM2 and MYD88 mutations in patients with chronic lymphocytic leukemia. *Oncol Lett* **17:** 4016–4023. doi:10.3892/ol.2019.10048

Mao S, Li Y, Lu Z, Che Y, Huang J, Lei Y, Wang Y, Liu C, Wang X, Zheng S, et al. 2019. PHD finger protein 5A promoted lung adenocarcinoma progression via alternative splicing. *Cancer Med* **8:** 2429–2441. doi:10.1002/cam4.2115

Matsuoka S, Ballif BA, Smogorzewska A, McDonald ER, Hurov KE, Luo JJ, Bakalarski CE, Zhao Z, Solimini N, Lerenthal Y, et al. 2007. ATM and ATR substrate analysis reveals extensive protein networks responsive to DNA damage. *Science* **316:** 1160–1166. doi:10.1126/science.1140321

Moiola C, De Luca P, Cotignola J, Gardner K, Vazquez E, De Siervi A. 2012. Dynamic coregulatory complex containing BRCA1, E2F1 and CtIP controls ATM transcription. *Cell Physiol Biochem* **30:** 596–608. doi:10.1159/000341441

Nimeth BA, Riegler S, Kalyna M. 2020. Alternative splicing and DNA damage response in plants. *Front. Plant Sci* **11:** 1–9. doi:10.3389/fpls.2020.00091

Paul A, Paul S. 2014. The breast cancer susceptibility genes (BRCA) in breast and ovarian cancers. *Front Biosci* **19:** 605–618. doi:10.2741/4230

Paulsen RD, Soni DV, Wollman R, Hahn AT, Yee MC, Guan A, Hesley JA, Miller SC, Cromwell EF, Solow-Cordero DE, et al. 2009. A genome-wide siRNA screen reveals diverse cellular processes and pathways that mediate genome stability. *Mol Cell* **35:** 228–239. doi:10.1016/j.molcel.2009.06.021

Pederiva C, Böhm S, Julner A, Farnebo M. 2016. Splicing controls the ubiquitin response during DNA double-strand break repair. *Cell Death Differ* **23:** 1648–1657. doi:10.1038/cdd.2016.58

Pleiss JA, Whitworth GB, Bergkessel M, Guthrie C. 2007. Rapid, transcript-specific changes in splicing in response to environmental stress. *Mol Cell* **27:** 928–937. doi:10.1016/j.molcel.2007.07.018

Polato F, Callen E, Wong N, Faryabi R, Bunting S, Chen H, Kozak M, Kruhlak MJ, Reczek CR, Lee W, et al. 2014. CtIP-mediated resection is essential for viability and can operate independently of BRCA1. *J Exp Med* **211:** 1027–1036. doi:10.1084/jem.20131939

Pollyea DA, Harris C, Rabe JL, Hedin BR, De Arras L, Katz S, Wheeler E, Bejar R, Walter MJ, Jordan CT, et al. 2019. Myelodysplastic syndrome-associated spliceosome gene mutations enhance innate immune signaling. *Haematologica* **104:** e388–e392. doi:10.3324/haematol.2018.214155

Polo SE, Jackson SP. 2011. Dynamics of DNA damage response proteins at DNA breaks: a focus on protein modifications. *Genes Dev* **25:** 409–433. doi:10.1101/gad.2021311

Prados-Carvajal R, López-Saavedra A, Cepeda-García C, Jimeno S, Huertas P. 2018. Multiple roles of the splicing complex SF3B in DNA end resection and homologous recombination. *DNA Repair (Amst)* **66–67:** 11–23. doi:10.1016/j.dnarep.2018.04.003

Rieger KE, Hong WJ, Tusher VG, Tang J, Tibshirani R, Chu G. 2004. Toxicity from radiation therapy associated with abnormal transcriptional responses to DNA damage. *Proc Natl Acad Sci* **101:** 6635–6640. doi:10.1073/pnas.0307761101

Savage KII, Gorski JJJ, Barros EMM, Irwin GWW, Manti L, Powell AJJ, Pellagatti A, Lukashchuk N, McCance DJJ, McCluggage WGG, et al. 2014. Identification of a BRCA1-mRNA splicing complex required for efficient DNA repair and maintenance of genomic stability. *Mol Cell* **54:** 445–459. doi:10.1016/j.molcel.2014.03.021

Shiozawa Y, Malcovati L, Galli A, Sato-Otsubo A, Kataoka K, Sato Y, Watatani Y, Suzuki H, Yoshizato T, Yoshida K, et al. 2018. Aberrant splicing and defective mRNA production induced by somatic spliceosome mutations in myelodysplasia. *Nat Commun* **9:** 3649. doi:10.1038/s41467-018-06063-x

Shkreta L, Chabot B. 2015. The RNA splicing response to DNA damage. *Biomolecules* **5:** 2935–2977. doi:10.3390/biom5042935

Shkreta L, Toutant J, Durand M, Manley JL, Chabot B. 2016. SRSF10 connects DNA damage to the alternative splicing of transcripts encoding apoptosis, cell-cycle control, and DNA repair factors. *Cell Rep* **17:** 1990–2003. doi:10.1016/j.celrep.2016.10.071

Soria-Bretones I, Sáez C, Ruíz-Borrego M, Japón MA, Huertas P. 2013. Prognostic value of CtIP/RBBP8 expression in breast cancer. *Cancer Med* **2:** 774–783. doi:10.1002/cam4.141

Soria-Bretones I, Cepeda-García C, Checa-Rodriguez C, Heyer V, Reina-San-Martin B, Soutoglou E, Huertas P. 2017. DNA end resection requires constitutive sumoylation of CtIP by CBX4. *Nat Commun* **8:** 113. doi:10.1038/s41467-017-00183-6

Spadaccini R, Reidt U, Dybkov O, Will C, Frank R, Stier G, Corsini L, Wahl MC, Lührmann R, Sattler M. 2006. Biochemical and NMR analyses of an SF3b155-p14-U2AF-RNA interaction network involved in branch point definition during pre-mRNA splicing. *RNA* **12:** 410–425. doi:10.1261/rna.2271406

Sum EYM, Peng B, Yu X, Chen J, Byrne J, Lindeman GJ, Visvader JE. 2002. The LIM domain protein LMO4 interacts with the cofactor CtIP and the tumor suppressor BRCA1 and inhibits BRCA1 activity. *J Biol Chem* **277:** 7849–7856. doi:10.1074/jbc.M110603200

Sun C. 2020. The SF3b complex: splicing and beyond. *Cell Mol Life Sci* **77:** 3583–3595. doi:10.1007/s00018-020-03493-z

Symington LS, Bizard AH, Hickson ID, Schiller CB, Seifert FU, Linke-winnebeck C. 2014. End resection at double-strand breaks: mechanism and regulation. *Cold Spring Harb Perspect Biol* **6:** a016436. doi:10.1101/cshperspect.a016436

Taricani L, Wang TSF. 2006. Rad4^{TopBP1}, a scaffold protein, plays separate roles in DNA damage and replication checkpoints and DNA replication. *Mol Biol Cell* **17:** 3456–3468. doi:10.1091/mbc.e06-01-0056

Teng T, Tsai JH, Puyang X, Seiler M, Peng S, Prajapati S, Aird D, Buonamici S, Caleb B, Chan B, et al. 2017. Splicing modulators act at the branch point adenosine binding pocket defined by the PHF5A-SF3b complex. *Nat Commun* **8:** 15522. doi:10.1038/ncomms15522

Tian J, Liu Y, Zhu B, Tian Y, Zhong R, Chen W, Lu X, Zou L, Shen N, Qian J, et al. 2015. SF3A1 and pancreatic cancer: new evidence for the association of the spliceosome and cancer. *Oncotarget* **6:** 37750–37757. doi:10.18632/oncotarget.5647

Veras I, Rosen EM, Schramm L. 2009. Inhibition of RNA polymerase III transcription by BRCA1. *J Mol Biol* **387:** 523–531. doi:10.1016/j.jmb.2009.02.008

Verma SP, Das P. 2018. Novel splicing in IGFN1 intron 15 and role of stable G-quadruplex in the regulation of splicing in renal cell carcinoma. *PLoS ONE* **13:** e0205660. doi:10.1371/journal.pone.0205660

Wu G, Lee WH. 2006. CtIP, a multivalent adaptor connecting transcriptional regulation, checkpoint control and tumor suppression. *Cell Cycle* **5:** 1592–1596. doi:10.4161/cc.5.15.3127

Xu J, Lv S, Qin Y, Shu F, Xu Y, Chen J, Xu BE, Sun X, Wu J. 2007. TRB3 interacts with CtIP and is overexpressed in certain cancers. *Biochim Biophys Acta* **1770:** 273–278. doi:10.1016/j.bbagen.2006.09.025

Yang T, Zhou H, Liu P, Yan L, Yao W, Chen K, Zeng J, Li H, Hu J, Xu H, et al. 2017. lncRNA PVT1 and its splicing variant function as competing endogenous RNA to regulate clear cell renal cell carcinoma progression. *Oncotarget* **8:** 85353–85367. doi:10.18632/oncotarget.19743

Yu X, Fu S, Lai M, Baer R, Chen J. 2006. BRCA1 ubiquitinates its phosphorylation-dependent binding partner CtIP. *Genes Dev* **20:** 1721–1726. doi:10.1101/gad.1431006

Zhao M, Zhuo M-L, Zheng X, Su X, Meric-Bernstam F. 2019. FGFR1β is a driver isoform of FGFR1 alternative splicing in breast cancer cells. *Oncotarget* **10:** 30–44. doi:10.18632/oncotarget.26530

Zheng Y-Z, Xue M-Z, Shen H-J, Li X-G, Ma D, Gong Y, Liu Y-R, Qiao F, Xie H-Y, Lian B, et al. 2018. PHF5A epigenetically inhibits apoptosis to promote breast cancer progression. *Cancer Res* **78:** 3190–3206. doi:10.1158/0008-5472.CAN-17-3514

Zhou W, Ma N, Jiang H, Rong Y, Deng Y, Feng Y, Zhu H, Kuang T, Lou W, Xie D, et al. 2017. SF3B4 is decreased in pancreatic cancer and inhibits the growth and migration of cancer cells. *Tumour Biol* **39:** 1010428317695913. doi:10.1177/1010428317695913